

Quantum Resistive Behaviors in the Vortex Liquid Regimes at Finite Temperatures

Ryusuke Ikeda

Department of Physics, Kyoto University, Kyoto 606-8502, Japan

(Dated: May 21, 2019)

Motivated by a *mean field-like* resistive behavior in magnetic fields commonly seen in various superconducting cuprates and organics with *strong* fluctuation, *quantum* superconducting (SC) fluctuation effects on resistive behaviors are reexamined by putting emphasis on their roles in the so-called *thermal* vortex liquid regime. By incorporating the quantum fluctuations and a vortex pinning effect in the Ginzburg-Landau (GL) fluctuation theory, it is found that the resistivity $\rho(T)$ -curve sharply drops, with no fan-shaped broadening, at a vortex-glass transition point far below an apparent upper critical field $H_{c2}^*(T)$ as a result of a quantum fluctuation enhanced by an adequately small condensation energy or by a strong field. Fittings to ρ - T data of cuprates and organics are performed by phenomenologically including a SC pseudogap region created by high energy SC fluctuations and possible fluctuations of competing non-SC orders. It is argued by performing fittings to $\text{La}_{2-x}\text{Sr}_x\text{CuO}_4$ data over a broad doping range that the in-plane coherence length of hole-doped cuprates decreases with approaching the underdoped limit *irrespective of* a coexistence of fluctuating competing orderings and that the condensation energy density $(H_c(0))^2 \sim [\phi_0/(2\pi\lambda(0)\xi_0)]^2$ is maximum near the optimal doping. Further, the case of disordered quasi 2D films showing the field-tuned superconductor-insulator transition (FSIT) is also examined for comparison and discussed in relation to data reported recently.

PACS numbers: 74.40.+k, 74.20.De, 74.72.-h, 74.60.-w

I. INTRODUCTION

Macroscopic behaviors in high temperature cuprate superconductors (HTS) in nonzero magnetic fields have led to a renewal of our knowledge on the superconducting (SC) fluctuation. In magnetic fields typically of tesla range, both the resistivity $\rho(T, H)$ and heat capacity in some optimally-doped HTSs have a field-induced fan-shaped broadening behavior below an *apparent* upper critical field $H_{c2}^*(T)$ (which will be defined later in this paper). Due to this consistency between ρ and thermodynamic quantities, the resistive broadening was explained as a generic phenomenon in a disordered state (thermal vortex liquid regime) created by the thermal SC fluctuation in nonzero fields[1, 2]. After that, the vortex lattice melting transition and its effect on the vanishing of Ohmic resistivity have been studied extensively[3, 4, 5] as key issues on the vortex phase diagram in real systems.

However, researches on the vortex phase diagram of HTS were limited to the case with low enough $H/H_{c2}^*(0)$ values, in which the fluctuation is purely thermal and the vortex pinning effect is weaker so that the discontinuous nature of the melting transition in pure case may remain intact. The corresponding measurement in larger $H/H_{c2}^*(0)$ values has been realized in overdoped HTSs under several teslas where effects of vortex-solidification are presumably negligible. Such materials seem to have a longer $T = 0$ in-plane coherence length ξ_0 , and their ρ - T curves have shown an apparently mean-field like sharp drop [6, 7]. Through a comparison with heat capacity data [8], however, it is clear at present that the resistivity drop in those materials has occurred much below $H_{c2}^*(T)$ possibly except at low enough temperatures, suggesting rather a strong fluctuation effect. The data in Refs.[6, 8]

may be understood assuming a purely thermal fluctuation and noting that the normal conductivity σ_n in the overdoped Tl-compounds is of the order $10^2(R_q d)^{-1}$ [6]. This value is much larger than a typical one of the vortex flow conductivity, i.e., the mean field expression of the superconducting part

$$\sigma_s = \sigma - \sigma_n \quad (1)$$

of the total conductivity σ , so that $\sigma \simeq \sigma_n$ (the normal part of σ) even much below $H_{c2}^*(T)$, where $R_q = \pi\hbar/2e^2 = 6.45$ ($\text{k}\Omega$) is the quantum resistance, and d the distance between the superconducting layers in a layered superconductor.

However, such a sharp drop of resistivity much below $H_{c2}^*(T)$ has been also observed in other cuprate superconductors [7, 9, 10, 11, 12] and also in organic superconductors [13, 14] with low $H_{c2}^*(T)$ but with much lower σ_n values ($< 10(R_q d)^{-1}$). It means that σ_s itself is extremely small in the thermal vortex liquid region in the tesla range of these materials, suggesting a strong SC fluctuation. Actually, it should be noticed that, in a high field, a longer ξ_0 does *not* necessarily imply a weaker fluctuation effect if recalling the fact that the fluctuation strength $g_2(H)$ in two dimensional (2D) systems near the zero field transition temperature $T_c(0)$ is given by [1]

$$g_2(H, T_c(0)) = \frac{16\pi^2\lambda^2(0)k_B T_c(0)}{\phi_0^2 d} \frac{H}{H_0} \propto T_c(0)(\lambda^2(0)\xi_0^2)H, \quad (2)$$

where ϕ_0 is the flux quantum, $\lambda(0)$ is the London penetration depth defined near $T_c(0)$, and $H_0 \equiv \phi_0/(2\pi\xi_0^2)$ is the *mean field* upper critical field at $T = 0$, where ξ_0 is the in-plane coherence length (A relation between H_0

and $H_{c2}^*(0)$ will be given later). According to eq.(2), an increase of ξ_0 under fixed values of other material parameters suggests an enhanced fluctuation at a fixed $H \neq 0$. Note that, in 2D limit, the Ginzburg number in $H = 0$ [4] corresponding to the above g_2 is independent of ξ_0 and given by $T_c(0)[\lambda(0)]^2/(\phi_0^2 d)$, except a constant prefactor, which decreases monotonically with overdoping in over (hole)-doped cuprates. As emphasized elsewhere [15], an increase of g_2 leads to an enhancement not only of the thermal fluctuation but of the *quantum* one. In contrast to the $H = 0$ case, the SC fluctuation in $H \neq 0$ remains noncritical even deep in the vortex liquid region, and thus, its quantum contribution may play an essential role there. In Fig.1, roles of quantum SC fluctuation in the resistivity are illustrated. Fig.1 (a) also includes a comparison with optimally-doped YBCO data [16]. If the *quantum* SC fluctuation is taken into account in addition to the thermal one, as the curves in Fig.1 show, an increase of g_2 (in this case, of $\lambda(0)$) results in a sharper drop of ρ - T curves at a 3D vortex-glass (VG) transition [3, 4] lying much below $T_{c2}^*(H)$ (corresponding to $H_{c2}^*(T)$). In Fig.1 (b), the filled circle on each solid curve indicates $T_{c2}^*(H)$. The sharp drop of ρ in Fig.1 (b) is in contrast to the case (Fig.1 (a)) dominated by the thermal fluctuation [1, 4], in which the resistivity starts to gradually decrease, more or less, around $H_{c2}^*(T)$, and is a combined effect of a (pinning-induced) 3D vortex glass transition and of a *reduction* of σ_s brought by the quantum fluctuations in the so-called *thermal* vortex liquid regime [3, 4]. It has been understood so far [4] that, in relation to the fluctuation effects in HTSs, the SC fluctuation in bulk materials with a large Ginzburg number near $T_c(0)$ and in $H \neq 0$ will be well described as the thermal fluctuation in the 3D XY model. Based on the above-mentioned fact, this conventional picture is invalid. The SC fluctuation in the limit of strong fluctuation is dominated by its quantum component, and the resistance follows the normal resistance even below $H_{c2}^*(T)$ without the fan-shaped broadening and shows a mean field-like sudden drop at a VG transition much below $H_{c2}^*(T)$.

The above-mentioned reduction of σ_s at relatively *high* temperatures is due to the same origin as the insulating $\sigma_s(T)$ in the *quantum* vortex liquid regime near $T = 0$ [15, 17]. However, in the temperature range where a pinning-induced VG fluctuation effect is negligible, a nearly classical (vortex flow-like) behavior intervenes these two quantum behaviors so that they can be conveniently seen as independent ones. In fact, the latter, i.e., a reduction of σ_s near $T = 0$, is limited in most cases to a very low temperature ($T/T_c(0) \ll 1$) window (see Fig.10 below) and is essential to understanding the field-tuned superconductor-insulator transition (FSIT) behavior [17] which cannot occur without quantum SC fluctuation. Further, thermodynamic quantities such as the magnetization at such a low T rapidly vary near $H_{c2}^*(T = 0)$ with sweeping H , reflecting [15] a rise of dimensionality of fluctuation on approaching $T = 0$. In contrast, the reduction of σ_s , i.e., the flattening of re-

sistance, in the thermal regime appears, as the example of Fig.1 shows, even at high temperatures comparable with $T_c(0)$ in systems with moderately strong fluctuation, and the corresponding T -dependence of thermodynamic quantities is broadened as the quantum fluctuation is stronger.

Roles of quantum fluctuation of vortex positions in a perfectly clean vortex solid have been examined by Blatter and Ivlev [18] as an explanation for high field behaviors of the first order melting line of clean vortex solid in optimally-doped YBCO. Note that the fluctuation of vortex positions is equivalent to the SC fluctuation because the vortex position are nodes (zero points) of the SC order parameter. However, it is well understood that the quantum effect on the melting transition of the optimally-doped samples is usually negligible. For instance, an observed field-induced deviation (reduction) of the melting line from the low field behavior is quite small and can be understood rather as a consequence of pinning disorder which is more effective with increasing fields [3]. On the other hand, the quantum fluctuation effect in the thermal vortex liquid regime has not been examined there [18]. Since the fluctuation with lower energy becomes more important upon cooling in the thermal vortex liquid regime (i.e., the disordered non SC phase), it is clear that the quantum fluctuation is much more important, e.g., near $H_{c2}^*(T)$ rather than near the melting line. As Fig.1 (a) shows, however, the quantum effect on the resistivity curves, and hence, on the melting transition line, of optimally-doped YBCO is quite negligible. When examining in this paper resistivity curves suggestive of a remarkable quantum fluctuation effect, the corresponding quantum effect on the VG transition line replacing the melting line [15] in clean limit is relatively negligible and will not be examined theoretically.

One might wonder if the flat or insulating resistance curves seen in cuprates may be explained based on the mean-field vortex flow conductivity and by assuming a friction coefficient (corresponding to the time scale γ in GL action defined in §2) to decrease upon cooling [20, 21]. Such a possibility might be argued for materials with an insulating $\sigma_n(T)$. However, the flat resistance curve is also seen in electron-doped and over (hole)-doped cuprates, where $\sigma_n(T)$ is metallic and tends to saturate upon cooling. Further, as is shown in §4, resistance curves in κ -(ET)₂ salts in high fields and at low temperatures have shown an insulating (and reentrant) T -dependence in spite of their metallic (saturating) $\sigma_n(T)$ behavior. This cannot be explained correctly within the mean-field theory based on the vortex flow conductivity.

This paper is organized as follows. First, in §2, a semi-quantitative theory describing resistivity curves in the thermal and quantum vortex liquid regimes is developed and, by incorporating microscopic details, used to fit experimental data in superconducting cuprates (§3) [19] and organics (§4) [22] in order to clarify that the rapid vanishing of resistance, often seen in these mate-

rial, is a consequence of a competition between a strong quantum SC fluctuation and 3D VG fluctuation. For comparison, the resistivity curves in disordered quasi 2D systems with *s*-wave pairing are also discussed in §5, and the transport energy U_ϕ , which is a similar quantity to the reversible magnetization at higher temperatures, is also calculated. As is argued in §3, when a strong SC fluctuation and/or a competing non-SC order parameter fluctuations are present near a mean-field transition temperature T_0 in $H = 0$, the width $T_0 - T_c(0)$ of a SC pseudogap region is broad and should be regarded as an independent material parameter in studying effects of fluctuation with *low* energy. In addition to data analysis in nonzero fields, effects of the SC pseudogap width and the quantum fluctuation on the critical region near $T_c(0)$ in $H = 0$ are also considered in §6, and these two ingredients are found to remarkably reduce the $H = 0$ critical region near $T_c(0)$.

II. EXPRESSION OF TRANSPORT QUANTITIES

We start with the 2D GL action expressed in terms of a single component pair-field $\psi(\mathbf{r}, \tau)$

$$S = d \int d^2r \left[\beta \sum_{\omega} (\psi_{\omega}(\mathbf{r}))^* \gamma(\mathbf{Q}^2) |\omega| \psi_{\omega}(\mathbf{r}) \right. \quad (3)$$

$$\left. + \int_0^{\beta} d\tau \left(u(\mathbf{r}) |\psi(\mathbf{r}, \tau)|^2 + (\psi(\mathbf{r}, \tau))^* \mu(\mathbf{Q}^2) \psi(\mathbf{r}, \tau) \right. \right. \\ \left. \left. + \frac{b}{2} |\psi(\mathbf{r}, \tau)|^4 \right) \right]$$

($\hbar, k_B = 1$), where $\psi(\tau) = \sum_{\omega} \psi_{\omega} e^{-i\omega\tau}$, β the inverse temperature, τ the imaginary time, and $b > 0$. The random potential $u(\mathbf{r})$ has zero mean and satisfies $\overline{u(\mathbf{r}) u(\mathbf{r}')} = b_p(\mathbf{r} - \mathbf{r}')$. Although the nonlocality of $b_p(\mathbf{r})$ is not negligible in $T \rightarrow 0$ limit [17], we assume that $b_p(\mathbf{r})$ can be replaced hereafter by $\delta(\mathbf{r} - \mathbf{r}')$ multiplied by a coefficient b_p because the quantum fluctuation effects in the thermal vortex liquid regime are primarily considered in this paper. Further, although the 3D nature due to the coupling between SC planes was neglected in writing eq.(1.1) because nearly 2D systems with strong anisotropy are primarily considered, it will be included later in considering a VG contribution to the conductivity. An additional dynamical term $i\gamma' \omega [\psi_{\omega}]^* \psi_{\omega}$ leading to a fluctuation Hall effect and resulting from a particle-hole assymmetry was neglected in eq.(3). This is justified as far as $|\gamma'| \ll \gamma$.

When the GL approach is applied to the low T and high H region in which any phase-only approach is inapplicable, H -dependences of the coefficients γ , μ , and b need to be taken into account since the familiar low T divergences [23] of these coefficients in zero field are cut off by the orbital depairing effect of the magnetic field. Although, strictly speaking, the Pauli paramagnetic depairing effect also suppresses the low T divergences, it

will be assumed that it becomes important only in much higher fields than the field range which is focused on in the present work. By expanding ψ in terms of the Landau levels (LLs) $\psi(\mathbf{r}) = \sum_n \varphi_{n,p} u_{n,p}(\mathbf{r})$, where $n (\geq 0)$ is the LL index, p is a quantum number measuring the degeneracy in each LL, and $u_{n,p}$ is an eigenfunction in n -th LL, the coefficients of quadratic terms of eq.(3) become n -dependent. For instance, the *bare* fluctuation propagator $\mathcal{G}_n^{(0)}(|\omega|) = \langle |\varphi_{n,p}(\omega)|^2 \rangle$ valid in $b, b_p \rightarrow 0$ limit is expressed by $\mathcal{G}_n^{(0)}(|\omega|) = (\gamma_n |\omega| + \mu_n)^{-1}$. The microscopic mean field transition point $T_0(H)$ (or $H_0(T)$) is defined by $\mu_0 = 0$. Detailed forms of γ_n and μ_n will be given separately in the following sections. On the other hand, no n -dependence of the coefficients b and b_p need to be specified throughout this paper, since a high H approximation is invoked below in obtaining expressions useful for analyzing experimental data, and hence, the interactions between the SC fluctuations or between a fluctuation and the random potential u are considered just within the LLL with $n = 0$. In particular, in examining the data of cuprates and organics in which microscopic descriptions are still controversial, it is appropriate to assume that b is one of material parameters and given by the magnetic penetration depth $\lambda(0)$ defined near $T_c(0)$, while the pinning strength b_p is a unknown fitting parameter.

To renormalize the ψ -fluctuation with low energy, the lowest LL approximation will be used. That is, it is assumed by invoking relatively high fields that the (renormalized) masses of higher ($n \geq 1$) LL fluctuations are heavy and almost the same as their bare ones, which are insensitive to T , and hence that the renormalization of higher LL modes has already been accomplished independently. Further, following previous works [3, 17], the vortex pinning effect in the LLL-fluctuation renormalization is incorporated to the one loop order. Then, the LLL fluctuation propagator $\mathcal{G}_0(|\omega|)$ is expressed in the form

$$(\mathcal{G}_0(|\omega|))^{-1} = \gamma_0 |\omega| + \mu_0 + \Delta\Sigma_h \quad (4)$$

$$+ \Sigma_0 + \Delta\Sigma_l - \frac{\tilde{b}_p}{2\pi r_B^2 d} \mathcal{G}_0(|\omega|)$$

(see also Fig.2). Here the factor \tilde{b}_p is a renormalized pinning vertex, sketched in Fig.2 (d), and is given by

$$\tilde{b}_p = r_B^2 b_p \int \frac{d^2k}{2\pi} e^{-\mathbf{k}^2/2} (1 + u_v e^{-\mathbf{k}^2/2})^{-2} = b_p / (1 + u_v), \quad (5)$$

where $u_v = b\beta^{-1} \sum_{\omega} \mathcal{G}_0^2(|\omega|) / (2\pi r_B^2 d)$. Consistently with this approximation, the VG transition point defined in the Gaussian approximation of VG fluctuation (i.e., the mean field VG transition point) is determined by the limit $t_{g,0} \rightarrow +0$, where

$$t_{g,0} = 1 - \tilde{b}_p [\mathcal{G}_0(0)]^2 / (2\pi r_B^2 d). \quad (6)$$

Although, strictly speaking, this pinning-renormalization is merely valid far above the vortex-solidification line in

the pinning-free limit [3] and is diagrammatically consistent just with the pinning-free fluctuation renormalization in the case with no $\Delta\Sigma_l$ (see below regarding $\Delta\Sigma_l$), this approximation will be used hereafter for practical purposes because all resistivity data we will examine below belong to the dirty case in the sense that they show no remnant of the first order vortex solid-liquid transition.

The main roles of LLL mass renormalization are played by the Hartree term Σ_0 of the self energy, which corresponds to Fig.2 (a), and is expressed as

$$\Sigma_0 = \frac{b}{2\pi r_B^2 d\beta} \sum_{\omega} \mathcal{G}_0(|\omega|). \quad (7)$$

We note that, in the ordinary low H and high T (the so-called GL-) region, the coefficient b is given by the familiar expression [1] $16\pi^2\lambda(0)^2/(\phi_0 H_0)$. Regarding the additional renormalization (correction) term $\Delta\Sigma_l$ within the lowest LL, an RPA type of approximation

$$\Delta\Sigma_l = \beta^{-1} \sum_{\omega} \mathcal{G}_0(|\omega|) \frac{\ln[1 + bE_{00}(|\omega|)/(\pi r_B^2 d)]}{2E_{00}(|\omega|)}, \quad (8)$$

(see eq.(2.11) of Ref.[15] and Fig.2 (b)) will be useful below, where $E_{00}(|\Omega|) = \beta^{-1} \sum_{\omega} \mathcal{G}_0(|\omega|) \mathcal{G}_0(|\omega + \Omega|)$. The term $\Delta\Sigma_l$ is negligible in the thermal 2D case [1] and, as far as a qualitative study of resistivity curves is concerned, will be negligible even in the quantum 2D case. However, to make sure, this term will be included when attempting to examine resistivity data in §3 and 4.

The term $\Delta\Sigma_h$ implies higher LL contributions to the LLL mass renormalization. It should be remarked [24] that the higher LL fluctuations are not negligible even in the present high H approximation but do contribute to a shift from $T_0(H)$ to the apparent mean field transition temperature $T_{c2}^*(H)$, just like in the zero field case [25] where the shift $T_0(0) - T_c(0)$ is ascribed to the amplitude-dominated fluctuation with *high* energy, and is conveniently represented by the Hartree diagram of the self energy (see Fig.2 (c)). It is clear that this definition on the normal-Meissner transition point implies that $T_c(0)$ mentioned above corresponds not to the true SC transition point at which the linear resistance vanishes but, roughly speaking, to an onset of a sharp resistive vanishing. This resistive onset, denoted as T_{c0} hereafter, is what appears in the ensuing expressions for $H \neq 0$. Since, when the quantum fluctuation is included, Fig.2 (c) is ultraviolet divergent even in 2D case, its H -dependence is a correction, and hence, $\Delta\Sigma_h$ may be identified with its expression in $H = 0$ case. Further, when the presence of other non-SC order parameter fluctuations coupling to the SC fluctuation is not negligible as in the underdoped cuprates, they may also be incorporated into $\Delta\Sigma_h$. It will be argued in §3 that even such non-SC fluctuation do not bring additional H -dependences. Then, $\Delta\Sigma_h$ may be written as $\ln(T_0/T_{c0})$ [15, 24], and the *effective* upper critical field $H_{c2}^*(T)$ (or equivalently $T_{c2}^*(H)$), defined consistently with T_{c0} , is determined by $\mu_0 + \Delta\Sigma_h = 0$.

Due to the presence of the pinning term $\propto \tilde{b}_p$, solving eq.(4) selfconsistently requires not a difficult but a very cumbersome numerical-integration even if neglecting $\Delta\Sigma_l$. A more cumbersome situation is encountered [17] when trying to present a practical expression on the VG contribution σ_{vg} to the conductivity. Since providing a theoretical formula useful in analyzing experimental data is one of purposes in this paper, we will not try to give a selfconsistent solution of eq.(4) but give below a practically more useful formulation on the LLL mass-renormalization by neglecting any pinning-induced renormalization of frequency dependences. That is, the form $\mathcal{G}_0(|\omega|) = (\gamma_0|\omega| + (\mathcal{G}_0(0))^{-1})^{-1}$ is assumed together with

$$(\mathcal{G}_0(0))^{-1} = \mu_0 + \ln(T_0/T_c(0)) + \Sigma_0 + \Delta\Sigma_l - \frac{\tilde{b}_p}{2\pi r_B^2 d} \mathcal{G}_0(0). \quad (9)$$

Consistently with this, Σ_0 and $E_{00}(\omega)$ are represented, respectively, as

$$\Sigma_0 = \frac{b}{2\pi^2 r_B^2 d \gamma_0} \int_0^{\epsilon_c} d\epsilon \coth\left(\frac{\beta\epsilon}{2\gamma_0}\right) \frac{\epsilon}{\epsilon^2 + (\mathcal{G}_0(0))^{-2}}, \quad (10)$$

where the cutoff ϵ_c is a constant of order unity, and

$$E_{00}(|\Omega|) = \beta^{-1} \sum_{\omega} \mathcal{G}_0(|\omega| + |\Omega|) \mathcal{G}_0(|\omega|) \times \left(1 + \frac{\gamma_0|\Omega|}{2} \mathcal{G}_0(|\Omega|/2)\right) \quad (11)$$

(see eq.(2.10) of Ref.[15]). Although, strictly speaking, this simplification is valid when $1 - t_{g,0} \ll 1$, its justification should be discussed through a fitting to experimental data. Through computations shown in the sections which follow, we found that refining this approximation was not necessary except at low enough temperatures in *s*-wave disordered films.

Transport quantities will be examined below in terms of Kubo formula for them. The superconducting part σ_s of the electric (diagonal) conductivity is written in the form

$$d \sigma_s = \left(-\frac{\partial}{\partial \Omega} \right) \overline{\langle j_{e,x}(-i\Omega) j_{e,x}(i\Omega) \rangle} \Big|_{\Omega \rightarrow +0}, \quad (12)$$

and the corresponding expression of the transport entropy is s_{ϕ} [26]

$$d s_{\phi} = \beta \phi_0 \left(-\frac{\partial}{\partial \Omega} \right) \overline{\langle j_{e,x}(-i\Omega) j_{h,y}(i\Omega) \rangle} \Big|_{\Omega \rightarrow +0}, \quad (13)$$

where the overbar implies the random average. The electric and heat currents in the low field GL region are given by

$$j_{e,x} = \xi_0^2 \frac{2\pi}{\phi_0} \psi^* Q_x \psi + \text{c. c.}, \quad (14)$$

$$j_{h,y} = \xi_0^2 i \partial_t \psi^*(t) Q_y \psi(t) + \text{c. c.}$$

respectively, where t is the real time, and \mathbf{Q} is the gauge-invariant gradient $-i\nabla + 2\pi\mathbf{A}/\phi_0$. The ensemble average is taken under the action (3) in type II limit with no \mathbf{A} fluctuations.

Within the high H approximation in which the spatially-averaged \mathbf{j}_e , $\langle \mathbf{j}_e \rangle_{\text{sp}}$, consists of the LLL and the next lowest LL, $\langle \mathbf{j}_e \rangle_{\text{sp}}$ is written as

$$\langle \mathbf{j}_e \rangle_{\text{sp}} = \frac{\pi r_B^2}{\phi_0} (\mathcal{G}_1(0))^{-1} \beta^{-1} \langle \psi^* (\mathbf{Q}\psi) + (\mathbf{Q}\psi)^* \psi \rangle_{\text{sp}}. \quad (15)$$

As shown in Ref.[17] (see eq.(2.23) there), the fact that the prefactor of \mathbf{j}_e is expressed in a vortex liquid region by the *renormalized* mass $(\mathcal{G}_1(0))^{-1}$ of the next lowest ($n = 1$) LL is independent of microscopic details and a consequence of gauge-invariance. In contrast, the prefactor of j_h may be, at least at low T/T_0 , strongly affected by a microscopic mechanism independent of the fluctuation property, and the vanishing s_ϕ in $T/T_0 \rightarrow 0$ limit results in. This issue in the s -wave case can be seen in Ref.[27].

Derivation of σ_s in the pinning-free limit, denoted hereafter as σ_f , was previously explained [3, 15]. As already mentioned, the higher LLs are assumed to be inert in the LLL mass-renormalization by invoking a situation in high H or deep in the vortex liquid regime. Consistently with this, any vertex corrections accompanied by an interaction between the LLL modes and the next lowest LL one can be neglected in the σ_f -expression. Then, our calculation of σ_f is the same as that in the Hartree approximation, and we obtain [15]

$$\begin{aligned} dR_q \sigma_f &= \frac{\gamma_0}{2(\mathcal{G}_1(0))^2 \beta} \sum_{\omega} \left[\mathcal{G}_0(\omega) \mathcal{G}_1(\omega) (\mathcal{G}_0(\omega) \right. \\ &\quad \left. + g \mathcal{G}_1(\omega)) - \frac{(\mathcal{G}_0(\omega))^2 + g^2 (\mathcal{G}_1(\omega))^2}{(\mathcal{G}_1(0))^{-1} + g (\mathcal{G}_0(0))^{-1}} \right] \\ &= (\mathcal{G}_1(0))^{-2} \int \frac{d\epsilon}{2\pi} \frac{\beta \gamma_0 \gamma_1 \epsilon^2}{2 \sinh^2(\beta \epsilon/2)} \\ &\quad \times \frac{1}{(\gamma_0^2 \epsilon^2 + (\mathcal{G}_0(0))^{-2})(\gamma_1^2 \epsilon^2 + (\mathcal{G}_1(0))^{-2})}, \end{aligned} \quad (16)$$

where $g = \gamma_1/\gamma_0$, and $\mathcal{G}_1(\omega) = (\gamma_1|\omega| + (\mathcal{G}_1(0))^{-1})^{-1}$. Note that the neglect of vertex corrections in σ_f based on the high H approximation does *not* conflict with the inclusion of $\Delta\Sigma_l$ in the mass renormalization.

In the realistic case with a vortex pinning, an additional contribution σ_{vg} to σ_s created by a pinning-induced vertex correction becomes divergent on approaching a 3D VG transition point T_{vg} [4, 28] from above. Near T_{vg} , the contribution of quantum SC fluctuation to σ_{vg} is negligible, and a σ_{vg} -expression in the thermal case

$$R_q d\sigma_{\text{vg}} = c_p \gamma_0 T_{c0} / (t - t_g)^s \quad (17)$$

will be used in comparing our theory with experimental data by choosing t_g and the prefactor c_p as being sample-dependent (i.e., pinning-dependent and, in the case of

cuprates, doping-dependent). Although the prefactor c_p should depend not only on b_p and b (i.e., the pinning and fluctuation strengths in $H = 0$) but on H [19], for simplicity, it will be assumed to be H -independent in §3 and 4. The exponent s is known to depend on the dimensionality of pinning potentials dominant in the sample we focus on, and, strictly speaking, it is difficult to predict an appropriate value of s through each fitting far above T_{vg} . In the fittings we have performed below, $s = 4.0$ was always assumed.

On the other hand, in situations where the system is 2D-like in spite of the presence of pinning effect, a true divergence of σ_{vg} may not occur, and hence the quantum fluctuation contribution to σ_{vg} is not negligible. As an approximate σ_{vg} -expression appropriate to this situation, the expression derived within the Gaussian approximation in Ref.[17]

$$\begin{aligned} R_Q d\sigma_{\text{vg}} &= \pi^{-1} \left(\frac{b_p \mathcal{G}_0(0)}{2\pi r_B^2 d} \right)^2 \beta^{-1} (\mathcal{G}_0(0))^{-2} \quad (18) \\ &\quad \times \sum_{\omega} \frac{\partial}{\partial |\omega|} \left[\ln(1 + c_c^{-2} \xi_{\text{vg},0}^2) \frac{\mathcal{G}_0(\omega)}{2} (\mathcal{G}_0(\omega) + \mathcal{G}_0(0)) \right. \\ &\quad \left. - (\mathcal{G}_0(\omega))^2 \ln \left(\frac{1 + c_c^{-2} \xi_{\text{vg},0}^2 + 2|\omega| \gamma_0 \mathcal{G}_0(0) [\xi_{\text{vg},0}]^4}{1 + 2|\omega| \gamma_0 \mathcal{G}_0(0) [\xi_{\text{vg},0}]^4} \right) \right] \end{aligned}$$

will be used below, where $\xi_{\text{vg},0}^2 = t_{\text{vg}}^{-1}$ is the dimensionless VG correlation length expressed in unit of r_B , and $t_{\text{vg}} = t_{\text{vg},0} + \sqrt{\gamma_0 T \mathcal{G}_0(0)}$. This form of t_{vg} is an expression useful for interpolation near an apparent 2D quantum VG transition field B_{vg}^* [17]. Further, the constant c_c is related to an upper cutoff of the wavevector integrals and will be hereafter chosen as $c_c = 1$. At B_{vg}^* defined by $t_{\text{vg},0}(B = B_{\text{vg}}^*, T = 0) = 0$, $\xi_{\text{vg},0}(T) \propto T^{-1/4}$, and $dR_q \sigma_{\text{vg}}(B = B_{\text{vg}}^*)$ is approximated by a *nonuniversal* [29] constant at low enough T where $\xi_{\text{vg},0} \gg 1$. Note that eq.(18) is an expression valid within the Gaussian approximation and hence, may diverge, as in 3D case, at a finite temperature. As is seen in §5, however, it is possible that it remains nondivergent at nonzero T , depending on the microscopic details. In the fittings, we will use either eqs.(17) or (18), depending upon the situations.

One might wonder if the fact that both of eqs.(16) and (18) vanish in low T limit is not a result of the neglect of the vertex corrections in the Kubo formulas. However, it was proved [15] at least in the pinning-free case that all terms including the vertex corrections vanish in low T limit. It is trivially performed to extend the proof in Ref.[15] to the case with vortex-pinning as follows. First, as in the electron systems [30], as far as the conductivity *prior to* the random average is considered, the *fluctuation* propagators $\mathcal{G}_n(|\omega|)$ ($n \geq 0$) depend on two coordinates and can be represented in a form like $\mathcal{G}_n(|\omega|; \mathbf{r}_1, \mathbf{r}_2) = \sum_{\mu} u_{\mu}(\mathbf{r}_1) \mathcal{G}_{n,\mu}(|\omega|) u_{\mu}^*(\mathbf{r}_2)$ where u_{μ} is an eigen function specified by a quantum number μ . Since the proof in Ref.[15] is applied in the same way as far as the spectral form (i.e., frequency dependence) in the low frequency

limit remains dissipative and is valid irrespective of the forms of coordinate or wavevector dependences of \mathcal{G}_n , the sum $\sigma_f + \sigma_{vg}$ is concluded to vanish in low T limit even if the vertex corrections are included. Therefore, by combining the high H approximation with this, the neglect of the vertex correction in eqs.(16) and (18) is safely valid.

Just as for the conductivity, the transport energy $U_\phi \equiv Ts_\phi$ may also be examined by neglecting the vertex

corrections in the Kubo formula because the heat current is also accompanied by the next lowest LL mode. On the other hand, the pinning-induced vertex correction related to the VG fluctuation may be neglected in s_ϕ assuming a weak pinning because no divergent contribution near T_{vg} arises in this quantity as a result of the additional time-derivative in the \mathbf{j}_h -expression. By arranging the frequency summation to take the Ω -derivative, we obtain

$$s_\phi = \frac{H}{dH_0(0)} (\mathcal{G}_1(0))^{-1} \sum_\omega \left[\gamma_0 \gamma_1 |\omega| ((\gamma_1 \mathcal{G}_1(0))^{-1} - (\gamma_0 \mathcal{G}_0(0))^{-1}) (\mathcal{G}_0(\omega) \mathcal{G}_1(\omega))^2 + \frac{1}{(\gamma_0 \mathcal{G}_0(0))^{-1} + (\gamma_1 \mathcal{G}_1(0))^{-1}} \right. \\ \left. \times \left[((\gamma_1 \mathcal{G}_1(0))^{-1} - (\gamma_0 \mathcal{G}_0(0))^{-1}) \mathcal{G}_0(\omega) \mathcal{G}_1(\omega) - \frac{\gamma_0}{\gamma_1} |\omega| (\mathcal{G}_0(\omega))^2 + \frac{\gamma_1}{\gamma_0} |\omega| (\mathcal{G}_1(\omega))^2 \right] \right]. \quad (19)$$

The $\omega = 0$ term of eq.(19) coincides with the thermal expression in Ref.[26]. In the present high H approximation, eq.(19) is simplified, by neglecting terms of higher order in $\gamma_1 \mathcal{G}_1(0) / (\gamma_0 \mathcal{G}_0(0))$, as

$$U_\phi \simeq \frac{\beta^{-1} H}{H_0 d \mathcal{G}_1(0)} \sum_\omega \mathcal{G}_1(\omega) \mathcal{G}_0(\omega) \simeq \frac{\phi_0^2}{16\pi^2 \lambda^2(0)} \Sigma_0, \quad (20)$$

where the prefactor $(\mathcal{G}_1(0))^{-1}$ is carried by an ET vertex. Namely, in the present high H approximation, s_ϕ in the GL region is proportional to the fluctuation entropy even in the quantum case, and the mean field result $\phi_0^2 \beta (1 - T/T_{c0}) / (16\pi^2 \lambda^2(0))$ is expected to be recovered deep in the vortex liquid regime if the fluctuation has calmed down there.

In the following sections, the above expressions of σ_f , σ_{vg} , and s_ϕ and eqs.(5), (8), (9), (10), and (11) are used together with an appropriate normal conductivity σ_n in fitting to experimental data of the resistivity

$$\rho = (\sigma_n + \sigma_f + \sigma_{vg})^{-1}, \quad (21)$$

where the normal conductivity σ_n is assumed to include other fluctuation conductivity terms excluded from the GL description, and of the Nernst coefficient

$$N = \frac{s_\phi \rho}{\phi_0}. \quad (22)$$

Independent material parameters are $\lambda(0)$, $T_0/T_c(0)$, H_0 , and $T_c(0)$ in addition to the σ_n -form. When the 3D σ_{vg} (16) is used, its prefactor and a form of transition line $t_g(H) = T_g(H)/T_{c0}$ are chosen to optimize the fittings. If the 2D form (18) is more applicable the pinning strength b_p is the only extrinsic fitting parameter.

III. CUPRATE SUPERCONDUCTORS

As an example of applying the formulation of §2 to analysis of experimental data, let us first examine re-

sistivity data in superconducting cuprates. Since one purpose of examining resistivity data of cuprates is to correctly understand the doping dependences of fluctuation effects and of material parameters of cuprates, we will primarily examine resistivity data of $\text{La}_{2-x}\text{Sr}_x\text{CuO}_4$ (LSCO) of which an extensive doping dependence can be seen in the literature [7]. As shown in Ref.[19] where the expressions obtained in §2 were used, data of other quantity measured consistently are also needed, together with resistivity data, to correctly estimate material parameters in cuprates with small condensation energy, and such a set of data in the underdoped regime are not known except the LSCO data in Ref.[31]. Below, we will proceed further the analysis in Ref.[19] to the overdope side and comment on other cuprate materials on the basis of available data [32, 33].

Most of resistivity data of cuprates in nonzero fields are those measured in several tesla. In the case of optimally-doped YBCO, ρ v.s. T curves in the field region show the fan-shaped broadening in the thermally-induced vortex liquid region below T_{c0} , and the thermal SC fluctuation reduces ρ -values at all temperatures except deep in the vortex liquid region. In Fig.1 (a), curves calculated in terms of σ_{vg} of eq.(17) are shown together with high field data in Ref.[16]. The parameters, except $\lambda(0)$ (see the caption of Fig.1), used in Fig.1 (a) and (b) are $\xi_0 = 1.1(\text{nm})$, $T_0 = 120(\text{K})$, $T_{c0} = 92(\text{K})$, $c_p = 1.3 \times 10^{-4}$, $\sigma_n^{-1} = 0.135T/T_{c0}(\text{m}\Omega\text{.cm})$, and $t_g = 1 - h - 1.2h^{2/3}$ with $h = H/H_{c2}^*(0)$. Since the h -values of optimally-doped YBCO in several teslas are much lower than those in LSCOs shown below, an additional contribution [1] composed only of *thermal* higher LL modes to σ_f was also included in obtaining the solid curves together with the quantum contribution accommodated in eq.(16). In Fig.1 (a), however, a change of resistivity value brought by the addition of higher LL contributions is within several percents in magnitude, and the quantum contribution was quite negligible. The ex-

tra higher LL contribution to σ_f in fields of several teslas is safely negligible in most of underdoped and overdoped materials and, regarding the LSCOs, at all doping levels, because they have a much lower $H_{c2}^*(0)$ than in optimally-doped YBCO. The positions of $H_{c2}^*(T)$ for each resistivity curve are denoted by filled circles both in Fig.1 (b) and the figures appearing hereafter. Further, the small but nonvanishing $T_0/T_{c0} - 1$ was taken into account here favoring an agreement with the consistent data of U_ϕ (see Fig.3).

In contrast to optimal YBCO, the $H_{c2}^*(T)$ -line in several teslas in materials with much lower $H_{c2}^*(0)$ is not necessarily approximated as a linear (straight) line, and we need a more reasonable functional form of $H_{c2}^*(T)$ at lower temperatures. To this end, we invoke the ordinary clean limit [34] in order to describe μ_n and γ_n consistently (see §2 on their definition). For simplicity, let us assume, as in the weak-coupling s -wave pairing case, a circular Fermi surface. This assumption will be commented on in §6. Then, they are given by

$$\gamma_n = \frac{\beta}{2\pi} \int_0^\infty ds \frac{s}{\sinh(s)} L_n(u_c^2 s^2) e^{-(u_c s)^2/2}, \quad (23)$$

$$\mu_n = \ln\left(\frac{T}{T_0}\right) + \int_0^\infty ds \frac{1 - L_n(u_c^2 s^2) e^{-(u_c s)^2/2}}{\sinh(s)},$$

respectively, where $u_c = T_0 \sqrt{H/(2H_0 e\gamma)}/T$, $L_n(x)$ is the n -th order Laguerre polynomial, and $\gamma = 0.5771$ is the Euler constant. Although, in the $d_{x^2-y^2}$ -pairing, cross terms between the lowest LL and the $n = 4m$ ($m \geq 1$) higher LLs arise in the quadratic terms of eq.(1), they can be safely neglected in situations of our interest where the lowest LL mode is dominant. It is valuable to comment on the fact that γ_n with any odd integer n approaches zero in $T \rightarrow 0$. Since an equilibrium vortex solid state is represented by the LLs with even n , a dissipative vortex flow motion is created by other odd LLs [24] so that the vortex flow conductivity is proportional to a γ_n with odd n . Hence, this result suggestive of dissipation-free vortex flow at $T = 0$ may be rather expected.

As noted in §2, the apparent or effective upper critical field line $H_{c2}^*(T)$ approaching T_{c0} in low H limit is determined by $\mu_0 + \Delta\Sigma_h = 0$. Using eq.(23), it is given by

$$H_{c2}^*(T) = H_0 \left(\frac{T_{c0}}{T_0} \right)^2 \Phi(t), \quad (24)$$

while the microscopic mean field transition field $H_0(T)$ is given by $H_0\Phi(T/T_0)$. Here, $t = T/T_{c0}$, and the function $\Phi(x)$ satisfies $\Phi(0) = 1$ and $\Phi(1) = 0$. In particular, when the parameter T_0/T_{c0} is large enough, this parameter significantly affects fluctuation phenomena in nonzero fields.

Note that, when T_{c0} rather than T_0 is chosen as a temperature parameter scaling T , H_0 is replaced by $H_{c2}^*(0) = H_0(T_{c0}/T_0)^2$. By combining this with eqs.(9) and (16), we find the property valid in the high H ap-

proximation

$$\sigma_f(T_{c0}, T_0/T_{c0}, H_0, \lambda(0)) = \sigma_f(T_{c0}, 1, H_{c2}^*(0), T_{c0}\lambda(0)/T_0). \quad (25)$$

Namely, if the SC pseudogap region existing over $T_0 - T_{c0}$ is neglected, $\xi_0 = \sqrt{\phi_0/(2\pi H_0(0))}$ is overestimated, while $\lambda(0)$ is underestimated. A discussion based on this fact will be given in §6.

We note that T_0 in the above expressions is the mean field SC transition point defined *prior to* including a coupling with possible non SC orderings competing with the SC ordering. We expect two types of origins of the SC pseudogap region $T_0 - T_{c0}$. First, a fluctuation of a competing non-SC ordering, such as a spin or charge ordering, coupling to the SC order parameter can lead to a reduction of T_0 . Since this can occur even at the mean field level where the SC fluctuation is entirely neglected, the resulting shift of T_0 corresponds to a shift of the $H = 0$ mean field (MF) transition temperature, and the resulting MF transition temperature will be called $T_c^{\text{MF}}(0)$ hereafter. This can be modelled by adding the term

$$\mathcal{S}_x = u_x \int_\tau \int d^2r |\phi_{ns}|^2 |\psi|^2 \quad (26)$$

in GL action, where ϕ_{ns} denotes a non-SC order parameter fluctuation, and only a fluctuation competitive (or repulsive) to ψ is assumed here through the condition $u_x > 0$. Since $|\phi_{ns}|^2$ is replaced by the averaged value $\langle |\phi_{ns}|^2 \rangle$ in constructing an effective action on ψ , $T_c^{\text{MF}}(0)$ will be expressed as $T_0 \exp(-u_x \langle |\phi_{ns}|^2 \rangle) / \langle T_0 \rangle$ by replacing $\ln(T/T_0)$ in μ_0 with $\ln(T/T_c^{\text{MF}}(0))$, where $\langle |\phi_{ns}|^2 \rangle$ was assumed to be H -independent. The second origin of T_0 -shift is nothing but $\Delta\Sigma_h$ in the LLL mass renormalization outlined in §2, where it was assumed to arise entirely from the SC fluctuation in higher LLs. An additional contribution to $\Delta\Sigma_h$ also arises from \mathcal{S}_x and similar higher order coupling terms between ψ and ϕ_{ns} . Assuming again this contribution to $\Delta\Sigma_h$ of such a ϕ_{ns} -fluctuation to be H -independent, $\Delta\Sigma_h$ can be identified with $\ln(T_c^{\text{MF}}(0)/T_{c0})$.

The assumption of H -independence of the ϕ_{ns} -fluctuation can be justified by comparing with experimental observations as follows. First, according to NMR measurements [35] in the pseudogap regime, the anti-ferromagnetic (AF) fluctuation with *low* energy, which is competitive with the SC fluctuation and should be dominant in the NMR signal in the nodal directions, is suggested to be insensitive to H at least in $T > T_{c0}$. On the other hand, the AF ordering was shown to be enhanced with increasing H primarily below the irreversibility line where the ohmic resistivity is absent [36]. This H -dependence of AF ordering is essentially linear in H , reflecting the number of vortices, and possibly, will be a consequence of the spatial variation of $|\psi|$ near the vortex cores [37, 38]. However, in the high H approach of GL theory, the spatial variation of $|\psi|$ is reflected only in $\beta_A - 1$ which is negligible [3]

in discussing thermodynamics and transport phenomena above the irreversibility line (i.e., in the vortex liquid regime). Therefore, we believe that the assumption of H -independence of ϕ_{ns} -fluctuation is valid in the vortex liquid regime. Even if the ϕ_{ns} -fluctuation carries an H -dependence in the effective action on the ψ -fluctuation, both fluctuations are competitive with each other, and hence, the resulting ξ_0 defined from a H -dependence in the effective action would be apparently enhanced. As is repeatedly seen hereafter, however, even the ξ_0 -values resulting from the fitting based on the neglect of H -dependences due to the ϕ_{ns} -fluctuation become short enough. For this reason, the extra H -dependence is likely to be quantitatively negligible. Therefore, we assume the contributions of ϕ_{ns} -fluctuation to be H -independent and to be fully accommodated as $\ln(T_0/T_c^{\text{MF}}(0))$. Although, as a result of this, $T_c^{\text{MF}}(0)$ does not appear in the r.h.s. of eqs.(4) and (9), the mean field transition field in the presence of ϕ_{ns} -fluctuations will be given by $H_0(T_c^{\text{MF}}(0)/T_0)^2\Phi(T/T_c^{\text{MF}}(0))$ which may decrease with underdoping. Note, nevertheless, that the intrinsic parameter ξ_0 is defined through the microscopic field scale H_0 irrespective of ϕ_{ns} -fluctuations.

Based on the inclusion, explained above, of competing ϕ_{ns} -fluctuations, the fitting results to LSCO x data with $x = 0.06$ and 0.08 reported in Ref.[19] will be commented on here. In Ref.[19], the formulas given in §2 were applied by neglecting the difference between T_0 and $T_c^{\text{MF}}(0)$. Regarding σ_{vg} , eq.(17) with $c_p = 10^{-2}$ was used for $x = 0.08$ case, and eq.(18) with $b_p = (2\pi\xi_0^2 d)0.023$ was applied to $x = 0.06$ case. According to the figures in Ref.[19], T_0 in $x < 0.1$ became insensitive to x there in contrast to T_ν , defined in Ref.[32] as the onset of SC Nernst signal, which *decreases* with decreasing x (< 0.1). Here, the fitting results to the $x = 0.08$ data given as Fig.2 in Ref.[19] will be shown again in Fig.4, where $(\sigma_n)^{-1} = 0.02905 \ln(1.6 \times 10^6 T_{c0}/T)$ (m Ω .cm) was assumed. Regarding the $x = 0.06$ case, it has been noticed later that, even if assuming T_0 to increase with decreasing x just like T_ν in Bi-compounds [32], the data can be quantitatively explained. For instance, the parameter values $\lambda(0) = 2.3(\mu\text{m})$, $T_0 = 100(\text{K})$, $T_{c0} = 13(\text{K})$, $H_0 = 493(\text{T})$, and $(\sigma_n)^{-1} = 0.0994 \ln(186.3 T_{c0}/T)$ (m Ω .cm) were used for the $x = 0.06$ case, and the obtained curves of ρ and N were almost the same as those in Fig.1 of Ref.[19] where $T_0 = 96(\text{K})$ was assumed. Contrary to this, no choice of T_0 decreasing with underdoping has resulted in a consistency with the Nernst data [31] particularly in the $x = 0.06$ case. What corresponds to T_ν in low H limit is the mean field transition point $T_c^{\text{MF}}(0)$. More accurately, because the Nernst signal due to *Gaussian* SC fluctuation is nonzero above the microscopic transition point, $T_c^{\text{MF}}(0)$ may lie slightly below T_ν . Hence, the unexpected doping dependence of T_ν in $x < 0.1$ will correspond to that of $T_c^{\text{MF}}(0)$ affected by competing non-SC fluctuations becoming stronger with underdoping. That is, we expect T_0 in LSCO to, like in Bi-compounds, increase with underdoping in contrast to

$$T_c^{\text{MF}}(0).$$

Next, in relation to Fig.4, the doping dependence of resistivity curves will be examined in order to argue that doping dependences of material parameters predicted in Ref.[19] are valid over a wider doping range including the overdoped side. Previously, a systematic study of resistive behaviors at various doping levels of LSCO was reported [7], and the data in Ref.[7] will be used here. We focus on the temperature range $10 < T(\text{K}) < 35$ and approximate each $[\sigma_n(T)]^{-1}$ curve there via a T -linear curve. Among various data in Ref.[7], we have examined three doping levels, $x = 0.08$ (underdoped case), $x = 0.15$ (nearly optimal case), and $x = 0.2$ (slightly overdoped case). First of all, the $x = 0.08$ data have been fitted by assuming a T_0/T_{c0} value similar to that in Fig.4. Next, the parameter values for $x = 0.2$ case were chosen by favoring a semiquantitative agreement with Nernst data in Ref.[39] (see Fig.1 there). Then, in $x = 0.15$ case, a T_0/T_{c0} value intermediate between the 0.08 and 0.2 cases was assumed. However, as mentioned in §2, the key parameter in comparing with ρ data is the product $\lambda(0)\xi_0$, or $H_c(0) = \phi_0/(2\sqrt{2}\pi\lambda(0)\xi_0)$ (see eq.(1)) which is independent of T_0 . The obtained curves are shown together with the data [7] in Fig.5, and the values of material parameters used for fittings are listed in Table.1, where α_g and β_g are the parameters included in the assumed form of VG transition curve $t_g(h) = T_g(h)/T_{c0} = (1 - h)/(1 + \beta_g h^{\alpha_g})$, and $h = H/H_{c2}^*(0)$.

In lower fields in $x = 0.08$, the resistivity curves have a fan-shaped broadening suggestive of a dominance of thermal fluctuation over the quantum contribution. One might wonder if the result in Fig.5 (a) that the thermal (fan-shaped) behavior in lower fields is more evident with underdoping is consistent with the argument [19] based on the data in *strongly* underdoped ($x < 0.1$) cases [31] where the thermal behavior was lost with underdoping in $x < 0.1$. This apparently conflicting result is resolved as follows. In the case of underdoped cuprates in tesla range, a strong SC fluctuation near T_0 is weakened to some extent upon cooling down to T_{c0} and behaves, much below T_0 , like that in effectively higher fields. Roughly speaking, the reduction of fluctuation arises from an increase upon cooling in $T_{c0} < T < T_0$ of the coefficient of the gradient term in the zero field GL-expression. That is, the enhanced quantum fluctuation due to $\lambda(0)$ increasing with underdoping is partly compensated by the existence of a large SC pseudogap region which, in turn, weakens the fluctuation near and below T_{c0} . Hence, an increase of $\lambda(0)$ may not necessarily result in a quantum fluctuation-dominated behavior near T_{c0} in the tesla range.

In Fig.5 (a), no $H_{c2}^*(T)$ position on the 29(T) curve was indicated. Actually, $H_{c2}^*(0)$ for Fig.5 (a) is close to 21(T), and hence, this 29 (T) curve is an example of the case in which the pinning-induced drop of resistivity occurs above $H_{c2}^*(T)$ as a consequence of a broad SC pseudogap region. It is not surprising because a VG transition can

occur anywhere in $T < T_0(H)$, i.e., as far as the SC fluctuation is present. This feature will be discussed again in §6.

In contrast, in $x = 0.2$ and 0.15 cases, the resistivity curves always show a sharp drop. As suggested in Ref.[39], the high field ρ curves in $x = 0.2$ case show a sharp drop far below $H_{c2}^*(T)$ suggested from Nernst data, and hence the situation is likely to be similar to Fig.1 (b) in Introduction. Actually, the much weaker H -dependence of ρ above T_{c0} in $x = 0.2$ than in $x = 0.15$ case is apparently inconsistent with an expected growth of ξ_0 with overdoping and rather suggests a fluctuation enhanced with overdoping. This is due to $\lambda(0)\xi_0$ increasing with overdoping, although the $H = 0$ fluctuation is weakened with overdoping (see §1). The U_ϕ -curves computed consistently with Fig.5 (c) are shown in Fig.6. The obtained U_ϕ values and H -dependences semiquantitatively agree with the data shown in Fig.1 of Ref.[39]. The properties of the curves are typically thermal, and, at least below 12 (T), there are no remarkable quantum fluctuation effect on U_ϕ . Regarding the $x = 0.15$ case, we note that the VG transition position $t_g(h)$ is closer to $H_{c2}^*(T)$ -line compared with those in $x = 0.08$ and 0.2 cases, and that, due to this, the sharp ρ -drop in $x = 0.15$ case is rather similar to that near $H_{c2}^*(T)$. This narrow vortex liquid regime suggested by the $x = 0.15$ data may occur if the *effective* pinning strength relative to the fluctuation strength is maximum near the optimal doping.

One of important consequences arising from the fittings is that $[H_c(0)]^{-1} \propto \lambda(0)\xi_0$, i.e., the fluctuation strength in $H \neq 0$ (see eq.(1)), is minimum near the optimal doping and increases with *both* underdoping and overdoping from the optimal case. This feature is comparable with the doping dependence of the estimated heat capacity jump $\Delta C \sim [H_c(0)]^2/T_{c0}$ and, actually, is qualitatively consistent with the doping dependence of condensation energy estimated from the heat capacity data [40]. Further, as Table I shows, the in-plane coherence length ξ_0 to be defined from H_0 monotonically decreases with underdoping over all doping ranges including $x < 0.1$ [19]. This conclusion cannot be reached once the presence of the SC pseudogap region widening with underdoping is neglected.

Examples of ρ and U_ϕ curves in a case with very large strengths of both the SC fluctuation and pinning effect are shown in Fig.7. They have been computed by bearing underdoped Bi-2201 data [33] with $T_{c0} \simeq 14$ (K) in mind. A quantitative comparison with the data will not be attempted here because the data were taken on a film sample with a broadening of $\rho(H = 0)$ curve over 10 (K). This sample-specific broadening at $H = 0$ should be also reflected in low H curves of resistivity and make comparison of computed curves with the low H data difficult. Nevertheless, we expect semiquantitative features of the Bi-2201 data except ρ -curves below 6(T) to be comparable with Fig.7. As well as the LSCO case with $x = 0.06$, the 2D σ_{vg} expression, eq.(18), was used. The parameters used in Fig.7 are $\lambda(0) = 1.9$ (μm),

$b_p = (2\pi\xi_0^2 d)0.15$, $T_0 = 6T_{c0}$, $T_{c0} = 15$ (K), $H_0 = 330$ (T), and $(\sigma_n)^{-1} = 0.21 \ln(280 T_{c0}/T)$ (m Ω .cm). Qualitatively, the features are similar to the 0.06 case of LSCO. First, the quantum SC fluctuation in Fig.7 is strong, and T_{c2}^* on the insulating ρ -curve at 8(T) is close to 5(K). More notably, the resistivity curves above 5(K) suggest a 2D FSIT near 6(T), just like Fig.1 of Ref.[19]. However, the FSIT behavior in Fig.7 is more remarkable compared to the LSCO case with $x = 0.06$ [19]. This is a consequence of the larger value of pinning strength b_p . Namely, a large enough value of pinning strength is needed *together with* a strong quantum SC fluctuation to obtain a more remarkable FSI transition behavior visible even near T_{c0} . On the other hand, the larger pinning effect enhances the VG transition field at low T . Actually, $H_{c2}^*(0)$ in Fig.7 is less than 10(T) at which a rapid drop of ρ at a finite T still occurs. Regarding the the transport energy, the U_ϕ -values in Fig.7 (b) should be compared with other figures of U_ϕ shown in this paper. As well as the LSCO case [19], the U_ϕ or N -values are two order of magnitude lower than a value expected when assuming no SC pseudogap region (i.e., $T_0 = T_c(0)$) and are consistent with the data [33].

This comparison with underdoped Bi-2201 data corroborates the argument in Ref.[19] based on the LSCO data as follows. Since, in contrast to the LSCO case in $x < 0.1$, T_ν in Bi2201 seems to monotonically increase [32] with underdoping, one might expect underdoped Bi-data to behave in a qualitatively different way from the LSCO data. On the other hand, as seen above, the present theory in which T_{c0}^{MF} corresponding to T_ν plays no essential roles explains the similarity in behaviors near and below T_{c0} of both ρ and U_ϕ data between Bi-2201 and LSCO. It implies that the examples of LSCO studied in Ref.[19] can be seen as generic behaviors of strongly underdoped cuprate materials below T_{c0} .

In this paper, the case of YBCO is not considered because no consistent data of ρ and N in underdoped YBCO have been reported. Further, the 3D nature of SC fluctuation should be incorporated in theoretical descriptions in contrast to other cuprates which are commonly much more 2d-like, and hence, the approach in §2 may not be directly applicable to a study of doping dependences of YBCO. Nevertheless, the doping dependences of T_ν and T_0 in YBCO should be clarified in future.

IV. ORGANIC SUPERCONDUCTORS

Previously, the resistive behaviors in the vortex liquid regime of κ -(ET)₂ organic superconductors have been studied in parallel with those of cuprate materials. Typical data are seen in Ref.[13, 14]. Surprisingly, the resistivity curves in κ -(ET)₂Cu(NCS)₂ with a wider vortex liquid regime have shown a sharp drop near the irreversibility line in all fields shown there. In κ -(ET)₂Cu[N(CN)₂]Br with a narrower liquid regime, the resistivity curves have shown a clear crossover induced by

the field H : In lower fields, the ρ - T curves show the familiar fan-shaped broadening, while the curves in higher fields follow the extrapolated normal resistivity σ_n^{-1} even much below $H_{c2}^*(T)$ estimated from the magnetization data and tend to drop sharply just above the irreversibility line. This cannot be understood based on the *thermal* fluctuation theory [1] which has succeeded in optimally-doped YBCO and Bi-2212. It has been noticed recently [19, 22] that this is a consequence of quantum SC fluctuation becoming more important as the fluctuation is stronger. Here, in addition to reproducing and discussing the fitting results reported elsewhere [22], the low T behaviors will be examined in order to clarify that the phenomena cannot be understood on the basis of the mean field vortex flow conductivity [20, 21] with an anomalously small friction coefficient.

Resistivity data of κ -(ET)₂Cu[N(CN)₂]Br [13] are fitted in terms of the present theory, and the results are shown in Fig.8 (a). The 3D form of σ_{vg} , eq.(16), is assumed, and the material parameters $\lambda(0) = 0.77(\mu\text{m})$, $T_0/T_c(0) = 1.2$, $T_c(0) = 12$ (K), $H_0 = 22$ (T), $d = 15$ (Å), and $c_p = 0.0035$ and the normal resistance $R_n(\Omega) = 0.0574 + 0.0243 t^{5/2}$ and $t_g = (1 - H/H_0)^2/(1 + 3.52(H/H_0)^{1/2})$ were used together with eq.(23). As a result of the large $\lambda(0)$ -value, the quantum SC fluctuation becomes essential with increasing H and leads to the sharp drop of $\rho(T)$ in high fields. For comparison, the U_ϕ curves obtained in terms of the same set of parameters are shown in Fig.8 (b). Note that, within the LLL, U_ϕ is equivalent to the magnetization, and hence that Fig.8 (b) can be also regarded as a typical example of thermodynamic quantity. A crossing behavior just below T_{c0} , which is familiar through magnetization data in many optimally-doped cuprate materials, is seen in lower fields below 2(T). It implies that the fluctuation property below 2(T) is purely thermal.

In contrast, the $U_\phi(T)$ -curve in 6(T) deviates from the crossing behavior in lower fields and is anomalously broadened, reflecting the stronger (quantum) fluctuation. Such an additional broadening of thermodynamic quantities (see the preceding paragraph) due to the quantum fluctuation is an opposite trend to the corresponding behavior near $T = 0$, where a broadening of such quantities becomes narrower reflecting a rise of dimensionality of SC fluctuation upon cooling [15]. This is why, as mentioned in §1, the quantum behavior at high temperatures should be distinguished from that near $T = 0$.

Next, the resistive behavior near $T = 0$ will be discussed based on the data of κ -(ET)₂Cu(NCS)₂ shown in Fig.9 which corresponds to Fig.3 of Ref.[41]. In the highest field 8.59(T) which is much above H_0 defined through a study of Shubnikov-de Haas effect [41], $\rho(T)$ shows a T -dependence indicative of a metallic normal state and approaches a residual value $\rho_n(0)$. In lower fields close to H_0 , $\rho(T)$ first decreases upon cooling as a result of thermal SC fluctuation, while it begins to increase on further cooling and approaches $\rho_n(0)$ (The ultimate drop at a low T of resistance below 7(T) will not be consid-

ered here). This insulating behavior occurs much below H_0 and hence, is a phenomenon of a SC origin. It is not permitted to ascribe this insulating behavior in a system with metallic normal resistance to, like the argument in Refs.[20, 21], a mean field vortex flow resistance with an insulating friction coefficient. The data in Fig.9 are direct evidences of the insulating behavior [42] arising from a purely dissipative quantum SC fluctuation in cases with metallic normal resistance. When the normal resistance is insulating as in the strongly underdoped cuprates and the s -wave dirty films (see §5), it is not easy to conclude a clear evidence of the insulating σ_f ($\sigma_f(T \rightarrow 0) \rightarrow 0$) in a case with dynamics dissipative at low T limit. For comparison, we give in Fig.10 examples of computed $\rho(T)$ curves with insulating behavior at low enough T arising from the quantum SC fluctuation. In Fig.10, the 2D σ_{vg} , eq.(18), was used, and the parameter values, $\lambda(0) = 1.1(\mu\text{m})$, $b_p = (2\pi\xi_0^2 d) 0.06$, $T_0 = T_{c0} = 25$ (K), and $H_0 = 19$ (T), were chosen. Further, the relations $(R_q d \sigma_n)^{-1} = 0.35(1 + 0.05(T/T_{c0})^{5/2})$ and $\mu_0 = T/T_{c0} - 1 + H/H_0$ were used, and, for simplicity, the vertex correction to the pinning strength was neglected by setting $\tilde{b}_p = b_p$.

V. s -WAVE DIRTY FILMS

In Ref.[17], we have proposed a theory of FSIT behavior in *homogeneously* disordered thin SC films with s -wave pairing on the basis of a familiar electronic model in dirty limit including effects of a repulsive mutual interaction between electrons. It has been argued there how, reflecting differences in T -dependences between various components in σ , the conductance value R_c on an apparent FSIT field B_c^* and the resistive behavior around B_c^* are affected by the normalized value R_n/R_q of the (high temperature) sheet resistance. However, no detailed computation results based on the GL action obtained microscopically were given there. Motivated by a recent finding on R_c v.s. R_n relation [43], some computed results on resistance curves consistent with the experimental observations [43, 44] will be presented here.

The parameters appearing in the GL action appropriate to the s -wave SC films were given in Ref.[17] and will be given here in a slightly modified manner. Among them, the parameters appearing in the quadratic terms of the GL action are given by

$$\begin{aligned} \mu_0 &= \ln(T/T_{c0}) + \sum_{n \geq 0} \frac{1}{(n + 1/2)((n + 1/2)\tilde{t} + 1)} \quad (27) \\ &\quad + \frac{R_n}{24\pi R_q} (\ln(2T_{c0}/(T + T_{cr}^{\text{mf}})))^3, \end{aligned}$$

$$\begin{aligned} (\mathcal{G}_1(0))^{-1} &\simeq \mu_1 - \mu_0 \quad (28) \\ &= 2\tilde{t} \sum_{n \geq 0} \frac{1}{(1 + \tilde{t}(n + 1/2))(3 + \tilde{t}(n + 1/2))}, \end{aligned}$$

and

$$\begin{aligned}\gamma_0 \simeq \gamma_1 &= \gamma^{(0)} / (1 + \frac{5R_n}{8\pi R_q} (\ln(2T_{c0}/(T + T_{cr}^{\text{mf}})))^2) \quad (29) \\ &= \frac{\tilde{t}}{4\pi T_{cr}^{\text{mf}}} \sum_{n \geq 0} (1 + \tilde{t}(n + 1/2))^{-2} \\ &\times (1 + \frac{5R_n}{8\pi R_q} (\ln(2T_{c0}/(T + T_{cr}^{\text{mf}})))^2)^{-1},\end{aligned}$$

where $T_{cr}^{\text{mf}} = 0.14T_{c0}H/H_{c2}^d(0)$, $H_{c2}^d(0)$ is H_0 in dirty limit, $\tilde{t} = T/T_{cr}^{\text{mf}}$, and γ_0 in dirty limit with no electron repulsion was denoted as $\gamma^{(0)}$. For simplicity, $\gamma_0 = \gamma_1$ was assumed because a difference between them is less important in dirty limit than that in clean limit (see eq.(23)) where γ_1 tends to vanish in $T \rightarrow 0$ limit. On the other hand, the coefficients b and b_p , respectively, of the interaction and pinning terms will be expressed as

$$b = \frac{r_B^2 dR_n}{3R_q} \frac{\tilde{t}}{T_{cr}^{\text{mf}}} \sum_{n \geq 0} (1 + \tilde{t}(n + 1/2))^{-3}, \quad (30)$$

and

$$\begin{aligned}b_p &= \left(\frac{r_B R_n}{R_q} \right)^2 \frac{d\tilde{t}}{6\pi} \sum_{n \geq 0} \sum_{m \geq 0} (n + m + 1)^{-1} \quad (31) \\ &\times (1 + \tilde{t}(n + 1/2))^{-1} (1 + \tilde{t}(m + 1/2))^{-1}.\end{aligned}$$

Here, the effects of electron-repulsion on b and γ_0 were included altogether just in γ_0 since its effect on γ_0 was estimated in Ref.[45] to be much larger than that in b , and they usually appears as the quantum fluctuation strength $\propto b/\gamma_0$ in the quantum regime. We note that b_p is $U_p f_{00}(0)$ in the notation of Ref.[17]. For simplicity, another parameter $2\pi T_{c0}\tau$, where τ denotes the elastic scattering time, was fixed to 0.5 through the computation.

As a normal conductivity σ_n for this case, the expression

$$R_q d\sigma_n = (1 - \frac{R_n}{3R_q} \frac{2\pi r_B^2 d\gamma^{(0)}}{b} \Sigma_0) / [1 + \frac{R_n}{4\pi R_q} \ln(T_{c0}/T)] \quad (32)$$

was used in the following figures, where Σ_0 is given by eq.(10). The second term of the numerator corresponds to the low T form, derived in Ref.[?], of additional quantum SC fluctuation contribution to σ_n excluded in the GL approach and was argued [17, 47] to be the origin of the *fluctuation-induced* [48] negative magnetoresistance in 2D and at low T .

Comments on the forms of log-corrections, resulting from the inclusion of electron-electron repulsive interaction, in μ_0 , γ_n , and σ_n will be necessary. The $T + T_{cr}^{\text{mf}}$ -dependence in μ_0 and γ_n was assumed as an interpolation between the expressions [49] in the two limits $T/H \rightarrow 0$ and $H/T \rightarrow 0$. Further, to represent $\ln(T_c(0)/T)$ -term in the denominator of σ_n ensuring $\sigma_n(T \rightarrow 0) \rightarrow 0$, a form of σ_n expected [50] in the case with a strong spin-orbit

scattering and with long-ranged Coulomb interaction was assumed as a model.

Applying the above microscopic parameters to eq.(9) and using eq.(18) as σ_{vg} , we have examined the resistivity curves near B_c^* in details. As a consequence of fixing the τT_{c0} value, the normalized sheet resistance (defined at high T) R_n/R_q is the only material parameter for our calculation of $R_q d\sigma$ and determines *both* strengths of quantum fluctuation and vortex pinning. Let us define B_c^* as the field at which $R(T)$ takes a value R_c insensitive to T at low enough T within the examined temperature range.

From the obtained curves shown in Fig.11, one will find the following two features on the curves near B_c^* . First, at lower values of R_n/R_q , the curves near B_c^* show an insulating T -dependence at intermediate temperatures, while they, for large R_n/R_q values, rather decrease upon cooling in the same temperature region. This feature has been seen in various data [51, 52, 53] and is nothing but the scenario predicted in Ref.[17]. At least within the present model of *s*-wave thin films, the decrease of R upon cooling for large enough R_n/R_q -values is dominated by an enhancement of pinning strength, while its increase in smaller R_n -values occurs primarily due to an enhancement of quantum SC fluctuation. For instance, the insulating $R(B \simeq B_c^*)$ for $R_n = 0.4R_q$ is controlled primarily by the quantum behavior of σ_f rather than σ_{vg} . Next, as listed in Table 2, R_c at lower R_n ($\leq 0.5R_q$) values roughly coincides with R_n , while R_c in $R_n \geq 0.6$ rather decreases with increasing R_n . The relation $R_c \simeq R_n$ at low disorder (lower R_n) coincides with the experimental results in $R_n \leq 5(\text{k}\Omega)$ summarized in Fig.4 of Ref.[44], while the saturation and reduction of R_c at higher disorder qualitatively agree with Fig.4 of Ref.[43].

Finally, we will comment on the validity of eq.(9) used in obtaining these figures on the basis of the microscopic informations listed above. When replacing eq.(4) with eq.(9), the pinning effect was underestimated. This simplification needs to be reconsidered in a close vicinity of a VG transition point (i.e., $t_{\text{vg},0} \rightarrow +0$). In trying to fit various data in §3 and 4, we did not have to discuss the details of resistivity data in the vicinity of the VG transition. In contrast, describing in details the resistive behaviors in 2D disordered thin films at low enough T and near B_c^* (i.e., near the quantum VG transition) is needed to clarify the physics of FSIT. We have partly carried out numerical computations based on eq.(4), although such a cumbersome analysis will not be presented here, and found that, roughly speaking, numerical results following from eq.(9) in $T/T_{c0} < 0.05$ in the cases of R_n/R_q -values used in Fig.11 are not reliable quantitatively. For this reason, no data in $T/T_{c0} < 0.05$ have been shown in Fig.11.

VI. COMMENTS AND DISCUSSION

First, an extended view over a wider temperature range of the resistivity curves in Fig.11 (b) is shown in Fig.12. From this figure, a $T = 0$ 2D VG transition point B_c^* is suggested to apparently lie much below $H_{c2}^*(0)$, because B_c^* itself is lowered by the quantum SC fluctuation [45], while the FSIT behavior appearing around B_c^* is a reflection of the VG fluctuation. Since the flat or insulating resistive behaviors appear in $H \geq B_c^*$, the temperature at which $R(T)$ drops in a field slightly below B_c^* *inevitably* lies far below $T_{c2}^*(H)$ indicated by a filled circle in the figure. Since the FSIT behavior is a consequence of strong quantum SC fluctuation, this example means that the sharp resistive drop much below $H_{c2}^*(T)$ in systems with strong quantum fluctuation is not an artifact of approximations we used in calculations but a generic feature irrespective of calculation methods of $R(T)$.

As shown in §3, the quantum fluctuation effect plays important roles in many cuprate materials under a high field. If the quantum SC fluctuation becomes essential, as in the example of Fig.1, due to a growth of $\lambda(0)$, one might expect the critical region width of the $H = 0$ transition, driven by the thermal fluctuation, to also widen due to the $\lambda(0)$ -growth. Actually, it was questioned in Ref.[32], through Figs.7 and 8 there, whether the pictures arguing a pseudogap of SC fluctuation origin are consistent with the fact that the critical region of the $H = 0$ transition, which can be conveniently expressed by $T_{c0} - T_c(0)$ (see §2) in our notation, does not widen much with underdoping. If the approach in §2 is extended to the $H = 0$ case, however, we find two theoretical facts to be explained below and believe them to satisfactorily explain the sharp $H = 0$ transition in underdoped cuprates. First, it is easily noticed that the quantum fluctuation itself reduces the width of critical region of the $H = 0$ transition at $T_c(0)$. To sketch the essence of this effect, we have only to examine a counterpart of eq.(4) (with $b_p = 0$) in the $H = 0$ case. In the isotropic 3D case, the renormalized mass μ_R (corresponding to $[\mathcal{G}_0(0)]^{-1}$) yields the relation

$$\mu_R - \ln(T/T_{c0}) = \sum_{\omega} [\sigma(\mu_R; \omega) - \sigma(0; \omega)], \quad (33)$$

where

$$\sigma(\mu_R; \omega) = 2\pi[\varepsilon_G^{(3)}(T)]^{1/2} \int_{\mathbf{q}} \frac{1}{\mu_R + q^2 + \gamma|\omega|}, \quad (34)$$

and $\varepsilon_G^{(3)}(T) = [16\pi^2(\lambda(0))^2/(\beta\xi_0\phi_0^2)]^2$ is the 3D Ginzburg number at temperature T . The thermal ($\omega = 0$) part of the r.h.s. becomes $-(\varepsilon_G^{(3)}(T))^{1/2}\sqrt{\mu_R}$. If keeping only this contribution in the r.h.s. and focusing on the low μ_R limit, the critical exponent $\nu = 1$ of the correlation length in the spherical limit is obtained. On the other hand, the ω -sum of other terms in the r.h.s. is $-\pi^{-2}\mu_R\sqrt{\varepsilon_G^{(3)}(\gamma^{-1})}$. The latter reduces a width of the

critical region which is usually defined by comparing the former with the μ_R in the l.h.s. of eq.(33). Actually, solving eq.(33), one finds the width of critical region to be estimated as $T_{c0}\varepsilon_G^{(3)}(T_c(0))/[16(1 + \pi^{-2}\sqrt{\varepsilon_G^{(3)}(\gamma^{-1})})]$, implying that, with decreasing γ , the critical region is narrower. The basic reason of this narrowing of the critical region due to the quantum fluctuation consists in the fact that the dimensionality of the dissipative quantum critical fluctuation at $T = 0$ in 3D case is five, which is above the upper critical dimension (four). The second origin leading to a narrowing of the $H = 0$ critical region is the broad SC pseudogap region $T_0 - T_{c0}$. By noting that the coefficient of the gradient term in $H = 0$ is nothing but that of the H -linear term in eq.(23), one easily finds that the 2D Ginzburg number *near* T_{c0} is given by $16\pi^2[\lambda(0)]^2k_B(T_{c0})^3/(\phi_0^2dT_0^2)$, where the reduction factor $(T_{c0}/T_0)^2$ is a consequence of *microscopic* T -dependence above T_{c0} . Within the approach in §2 where no specific origin leading to a reduction of the time scale γ is assumed, this second ingredient is dominant and seems to be adequate for understanding why the $H = 0$ critical region in underdoped cuprates is unexpectedly narrow.

In relation to the second ingredient mentioned above, we need to comment on the definition of penetration depth comparable with experimental data [54]. The actual penetration depth in $H = 0$ is defined as the mass of the gauge field through the gradient term. Hence, in our notation, the penetration depth to be observed near T_{c0} is not $\lambda(0)/(1-T/T_{c0})^{1/2}$ but $T_{c0}\lambda(0)/[T_0(1-T/T_{c0})^{1/2}]$. The former is the quantity to be observed as the penetration depth in $H = 0$ and at low T , where the fluctuation is negligible, if a T -dependence of the coefficient b in the SC pseudogap region can be neglected, because we have defined $\lambda(0)$ at a microscopic level. Thus, in underdoped materials with broader SC pseudogap region, the $[\lambda(T)]^{-2}$ v.s. T curve is not linear even approximately, and, as observed in Ref.[54], its local slope increases on approaching $T_c(0)$ from below. However, we note that the $\lambda(0)$ -values we have estimated by fitting are larger than those estimated experimentally [54]. If effects of the competing orders may be relatively negligible, the b -value near $T_c(0)$ will be, as well as γ_0 , larger than that near T_0 . Thus, the differences in $\lambda(0)$ -values obtained through Fig.5 from the experimental data [54] does not necessarily require modification of the present theory.

We emphasize that key data suggesting [14, 19, 31, 39] an "inconsistency" between the resistivity and the Nernst coefficient were explained without taking account of electronic structures peculiar to strongly correlated materials. This is in contrast to such an argument assuming a strong reduction of the friction coefficient, to which the *mean field* vortex flow conductivity is proportional, on the basis of a FS anisotropy [20] or of the absence of vortex core states [21]. As emphasized in Introduction and elsewhere [19], the "inconsistency" is not peculiar to underdoped cuprates but, according to Figs.8 and 12, appears even in the organic and *s*-wave materials.

In Fig.5 (a), we have included a $\rho(T)$ curve at 29(T) which is above $H_{c2}^*(0)$. The sharp drop of this curve near 10(K) indicates a 3D VG transition point above $H_{c2}^*(T)$. Since, in principle, the VG transition may occur as far as the SC fluctuation is present, such a 3D VG transition in the SC pseudogap region $T_{c2}^*(H) < T < T_0(H)$ may be present, in contrast to the scenario in Ref.[20] for the data [6], without a granularity in the sample.

It is interesting to connect the nonmonotonic doping dependence of $T_\nu(x)$ in LSCO to a sign change [55] of the fluctuation Hall conductivity $\sigma_{f,xy}$. It is now clear that a sign reversal of Hall conductivity, usually seen in the vortex liquid regime, may occur, depending on the materials, above $H_{c2}^*(T)$. It means that this Hall-sign reversal should be understood based on the fluctuation scenario [56] unrelated to the electronic states of vortex cores. According to this scenario, the sign of $\sigma_{f,xy}$ is determined by that of $\partial T_c^{\text{MF}}(0)/\partial x$, and hence, if T_ν is essentially identical with $T_c^{\text{MF}}(0)$, the sign change of $\partial T_\nu/\partial x$ should appear directly as that of $\sigma_{f,xy}$. According to Ref.[55], the LSCO data in $x \geq 0.12$ show a Hall-sign reversal, while available ρ_{xy} data in $x = 0.08$ [57] have not shown any sign reversal, consistently with our expectation. On the other hand, according to [12], the Hall data of very underdoped Bi2201 continue to show a sign reversal, consistently with the monotonic doping dependence of T_ν of this material (see Fig.10 in Ref.[32]). This is why the identification between T_ν and T_c^{MF} seems to be consistent with available Hall-resistance data.

In hole-doped cuprates, the positive magnetoresistivity in the SC pseudogap region above T_{c0} is enhanced with underdoping. Actually, this trend has led the authors in Ref.[58] to argue that ξ_0 increases with underdoping. This enhanced magnetoresistivity above T_{c0} can be seen as a reflection of the resistivity curves following the extrapolated normal curve even much below $T_{c2}^*(H) (< T_{c0})$. Actually, in a strong SC fluctuation case such that its quantum nature is no longer negligible, the Gaussian approximation for the SC fluctuation fails, and the interaction between the SC fluctuations should not be neglected even much above T_{c0} . Hence, the quantum SC fluctuation may be a main origin of the enhanced [58] magnetoresistance in the SC pseudogap region (i.e., $T_{c0} < T < T_0$). In any case, as demonstrated in Ref.[19], data analysis *only* of $\rho(T)$ curves in cases with low $H_c(0)$ and hence, with large quantum fluctuation tends to lead to an erroneous estimation of material parameters. A simultaneous study of other quantities, such as U_ϕ , measured consistently with ρ is indispensable. Further, the neglect of SC pseudogap region in thermodynamic quantities such as the magnetization [59] also seems to erroneously lead one to concluding a ξ_0 increasing with underdoping.

The author thanks T. Sasaki, C. Capan and W. Lang for providing him their unpublished data.

[1] R. Ikeda, T. Ohmi, and T. Tsuneto, J. Phys. Soc. Jpn. **60**, 1051 (1991).
[2] R. Ikeda, T. Ohmi, T. Tsuneto, Phys. Rev. Lett. **67**, 3874 (1991).
[3] R. Ikeda, J. Phys. Soc. Jpn. **65**, 3998 (1996).
[4] D. S. Fisher, M. P. A. Fisher, and D. A. Huse, Phys. Rev. B **43**, 130 (1991).
[5] T. Nattermann and S. Sheidl, Adv. Phys. **49**, 607 (2000).
[6] A. P. Mackenzie et al., Phys. Rev. Lett. **71**, 1238 (1993).
[7] M. Suzuki and M. Hikita, Phys. Rev. B **44**, 249 (1991).
[8] A. Carrington, A. P. Mackenzie, and A. Tyler, Phys. Rev. B **54**, R3788 (1997).
[9] S. Kleefisch et al., Phys. Rev. B **63**, 100507 (2001); F. Gollnik and M. Naito, Phys. Rev. B **58**, 11734 (1998).
[10] D. J. C. Walker et al., Phys. Rev. B **51**, 9375 (1995).
[11] K. Karpinska et al., Phys. Rev. Lett. **77**, 3033 (1996).
[12] S. I. Vedeneev et al., Phys. Rev. B **60**, 12467 (1999).
[13] T. Sasaki, unpublished. See also A. Matsuyama et al., Physica C **263**, 534 (1996).
[14] H. Ito et al., Physica B **201**, 470 (1994).
[15] R. Ikeda, Int. J. Mod. Phys. B **10**, 601 (1996).
[16] H. C. Ri et al., Phys. Rev. B **50**, 3312 (1994).
[17] H. Ishida and R. Ikeda, J. Phys. Soc. Jpn. **71**, 254 (2002) and 2352 (2002).
[18] G. Blatter and B. Ivlev, Phys. Rev. Lett. **70**, 2621 (1993).
[19] R. Ikeda, Phys. Rev. B **66**, 100511(R) (2002) (cond-mat/0203221).
[20] V. B. Geshkenbein, L. B. Ioffe and A. J. Millis, Phys. Rev. Lett. **80**, 5778 (1998).
[21] P. A. Lee and G. Sha, cond-mat/0209572.
[22] R. Ikeda, presented in Int. Conf. LT23 (to appear in Physica C).
[23] See, for instance, T. R. Kirkpatrick and D. Belitz, Phys. Rev. Lett. **79**, 3042 (1997).
[24] R. Ikeda, J. Phys. Soc. Jpn. **64**, 1683 (1995).
[25] B. I. Halperin and D. R. Nelson, J. Low Temp. Phys. **36**, 599 (1979). The temperature T_c^0 in this reference corresponds to T_{c0} in the present paper.
[26] R. J. Troy and A. T. Dorsey, Phys. Rev. B **47**, 2715 (1993).
[27] K. Maki, Physica (Utrecht) **55**, 125 (1971).
[28] R. Ikeda, J. Phys. Soc. Jpn. **66**, 1603 (1997).
[29] In contrast to the case of *s*-wave dirty films, the critical VG conductance value is *always* nonuniversal in general case where the parameters γ_0 , b_p , and b are independent of each other.
[30] P. W. Anderson, J. Phys. Chem. Solids **11**, 26 (1959).
[31] C. Capan et al., Phys. Rev. Lett. **88**, 056601 (2002).
[32] Y. Wang et al., Phys. Rev. B **64**, 224519 (2001).
[33] C. Capan, unpublished.
[34] P. A. Lee and M. G. Payne, Phys. Rev. B **5**, 923 (1972).
[35] V. F. Mitrovic et al., Phys. Rev. B **66**, 014511 (2002).
[36] B. Khaykovich et al., Phys. Rev. B **66**, 014528 (2002).
[37] S. A. Kivelson et al. cond-mat/0205228.
[38] E. Demler, S. Sachdev, and Y. Zhang, Phys. Rev. Lett. **87**, 067202 (2001).
[39] Y. Wang et al., Phys. Rev. Lett. **88**, 257003 (2002).
[40] J. W. Loram et al., Physica C **341-348**, 831 (2000).

- [41] T. Sasaki et al., cond-mat/0208124.
- [42] R. Ikeda, J. Phys.Soc.Jpn. **65**, 33 (1996).
- [43] E. Bielejec and W. Wu, Phys. Rev. Lett. **88**, 206802 (2002).
- [44] P. Phillips and D. Dalidovich, cond-mat/0104504.
- [45] H. Ishida, H. Adachi, and R. Ikeda, J. Phys. Soc. Jpn. **71**, 245 (2002).
- [46] V. M. Galitski and A. I. Larkin, Phys. Rev. B **63**, 174506 (2001).
- [47] R. Ikeda, Phys. Rev. Lett. **89**, 109703 (2002).
- [48] S. Okuma et al., Phys. Rev. B **63**, 054523 (2001).
- [49] H. Ishida and R. Ikeda, J. Phys. Soc. Jpn. **67**, 983 (1998).
- [50] P. A. Lee and T. V. Ramakrishnan, Rev. Mod. Phys. **57**, 287 (1985).
- [51] A. F. Hebard and M. A. Paalanen, Phys. Rev. Lett. **65**, 927 (1990).
- [52] J. A. Chervenak and J. M. Valles, Jr., Phys. Rev. B **61**, R9245 (2000).
- [53] V. F. Gantmakher et al., JETP Lett. **71**, 160 (2000).
- [54] C. Panagopoulos et al., cond-mat/9903117.
- [55] T. Nagaoka et al., Phys. Rev. Lett. **80**, 3594 (1998).
- [56] R. Ikeda, Physica C **316**, 189 (1999). See the footnote of the first page there.
- [57] W. Lang, private communication.
- [58] Y. Ando and K. Segawa, Phys. Rev. Lett. **88**, 167005 (2002).
- [59] M. Li et al., Phys. Rev. B **66**, 024502 (2002).

Fig.1 (a) Resistivity curves (solid lines) in 4, 8, and 12(T) calculated in terms of $\lambda(0) = 0.11(\mu\text{m})$ and 8 and 12 (T) data (symbols) in twinned optimally-doped YBCO [16] in 12(T). See §3 for the details of calculations and other parameter values used here. (b) Curves obtained using $\lambda(0) = 0.35(\mu\text{m})$ which correspond to the solid curves in (a). In this and other figures, each darkened circle on a $\rho(T)$ curve denotes T_{c2}^* in each field.

Fig.2 Diagrams expressing (a) Σ_0 , (b) $\Delta\Sigma_l$, (c) Σ_h , and (d) \tilde{b}_p . The vertex correction (the hatched rectangle) is expressed in the diagram (e). The solid lines, the solid dot, the chain line, and the dashed line with cross express, respectively, \mathcal{G}_0 , b , \mathcal{G}_n ($n \geq 1$), and b_p .

Fig.3 U_ϕ -curves (solid curves) and 12 (T) data (open squares) [16] corresponding to those in Fig.1 (a). In this

and other figures of $U_\phi(T)$, U_ϕ is represented in unit of $10^{-12}(\text{J/m})$.

Fig.4 Fittings to LSCO $x = 0.08$ data of (a) ρ and (b) N in Ref.[31].

Fig.5 Resistivity data (symbols) [7] of LSCO at the three doping levels (a) $x = 0.08$, (b) 0.15, and (c) 0.2 and corresponding theoretical results (solid curves).

Table 1 Material parameters used in calculations of Fig.5.

Fig.6 U_ϕ -curves corresponding to ρ -curves in Fig.5 (c).

Fig.7 (a) Resistivity curves and (b) U_ϕ -curves obtained by imagining underdoped Bi2201 data [33].

Fig.8 (a) Fitting results to resistivity data [13] of κ -(ET)₂Cu[N(CN)₂]Br and (b) the expected U_ϕ -curves corresponding to the solid curves in (a).

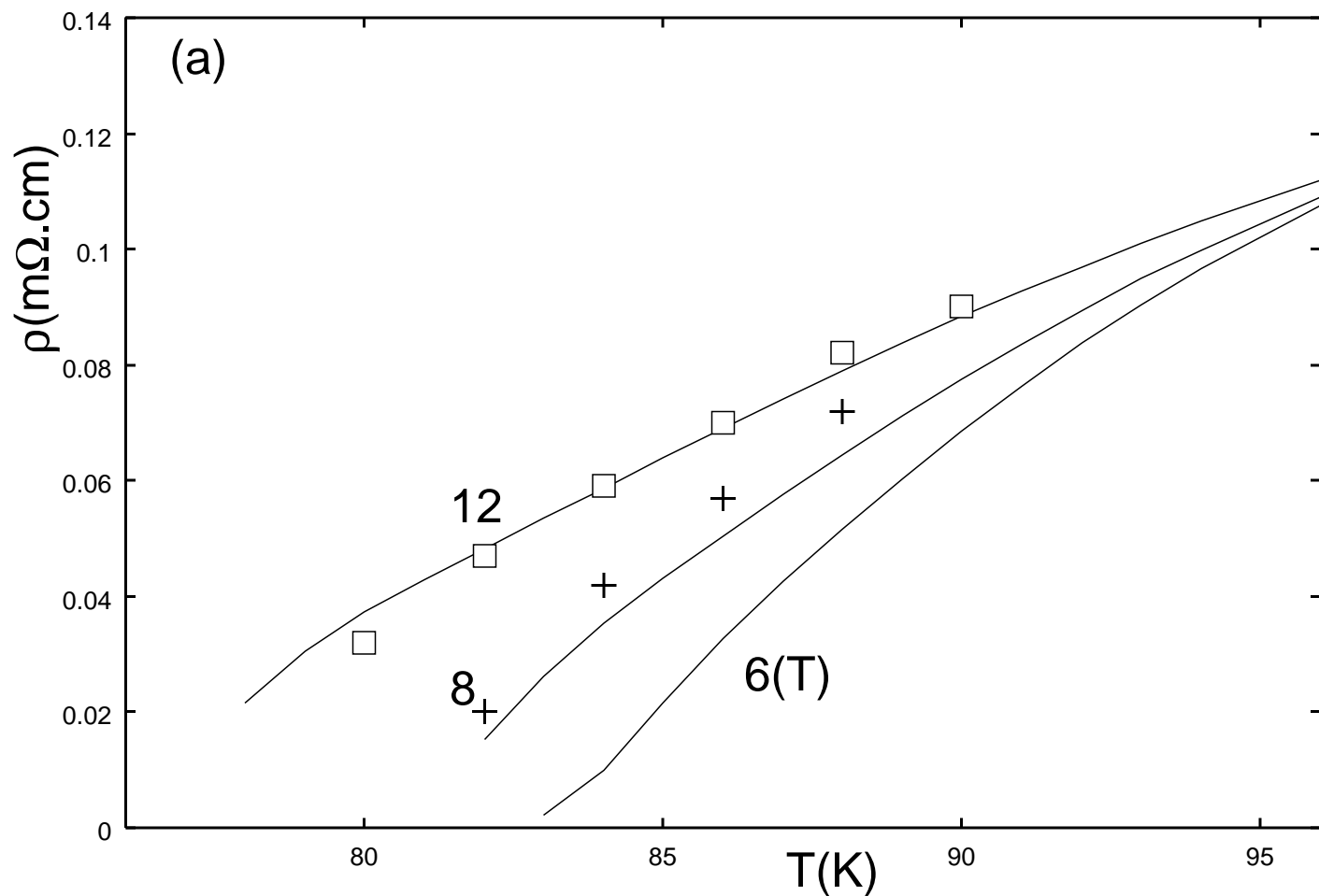
Fig.9 Data of resistivity of κ -(ET)₂Cu(NCS)₂ near $T = 0$ and in strong fields [41].

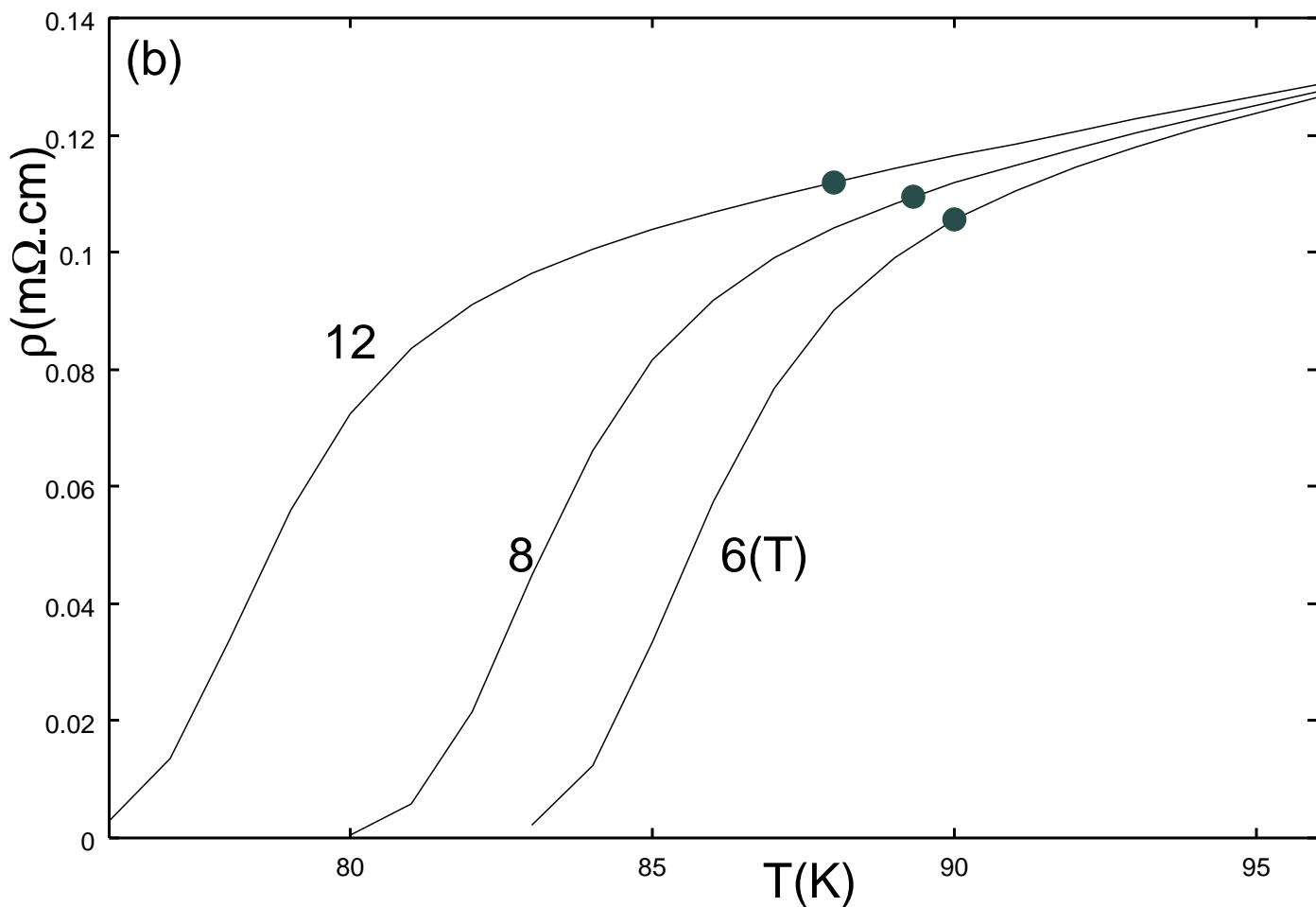
Fig.10 Resistivity curves computed for a qualitative comparison with the data in Fig.9.

Fig.11 Calculated resistivity curves imagining *s*-wave dirty films for three R_n/R_q values : (a) $R_n/R_q = 0.4$ in $h \equiv H/H_{c2}^d(0) = 0.87, 0.82, 0.79, 0.77, 0.76, 0.74, 0.7, 0.65$, and 0.6, (b) $R_n/R_q = 0.57$ in $h = 0.9, 0.85, 0.8, 0.75, 0.7, 0.67, 0.64$, and 0.6, and (c) $R_n/R_q = 0.67$ in $h = 0.9, 0.8, 0.67, 0.63, 0.61, 0.59, 0.55$, and 0.51.

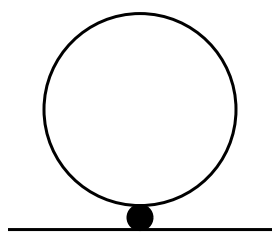
Table 2 R_n/R_q dependences of the normalized critical resistance R_c/R_n and of the normalized critical field $B_c^*/H_{c2}(0)$, estimated for each case of the calculated resistivity curves illustrated in Fig.11.

Fig.12 Extended view of Fig.11 (b) to higher temperatures. Here, a curve in $h = 0.4$ is added further.

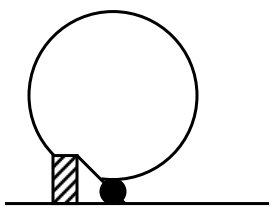




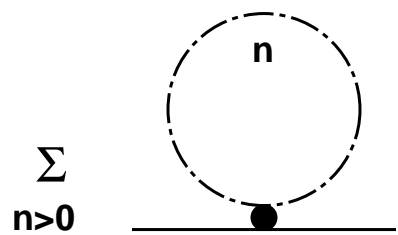
x	0.08	0.15	0.2
λ (μ m)	0.57	0.46	0.417
H_0 (T)	245	190	55.1
T_0 (K)	100	86.5	40.5
T_{c0} (K)	30	31	30
ρ_n ($m\Omega.cm$)	0.245 + 0.27 t	0.19 + 0.0426 t	0.055 + 0.0312 t
C_p	0.04	0.01	0.033
α_g	0.5	0.67	0.67
β_g	3.4	0.8	2.26
$H_c(0)$ (T)	0.352	0.385	0.229



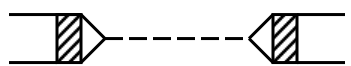
(a)



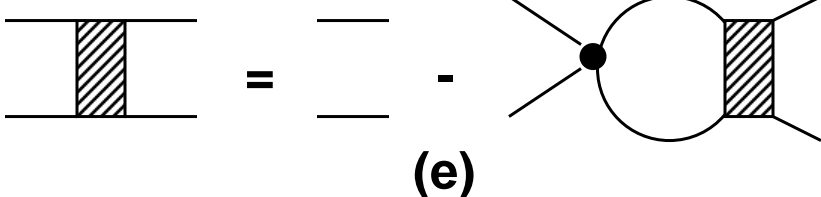
(b)



(c)

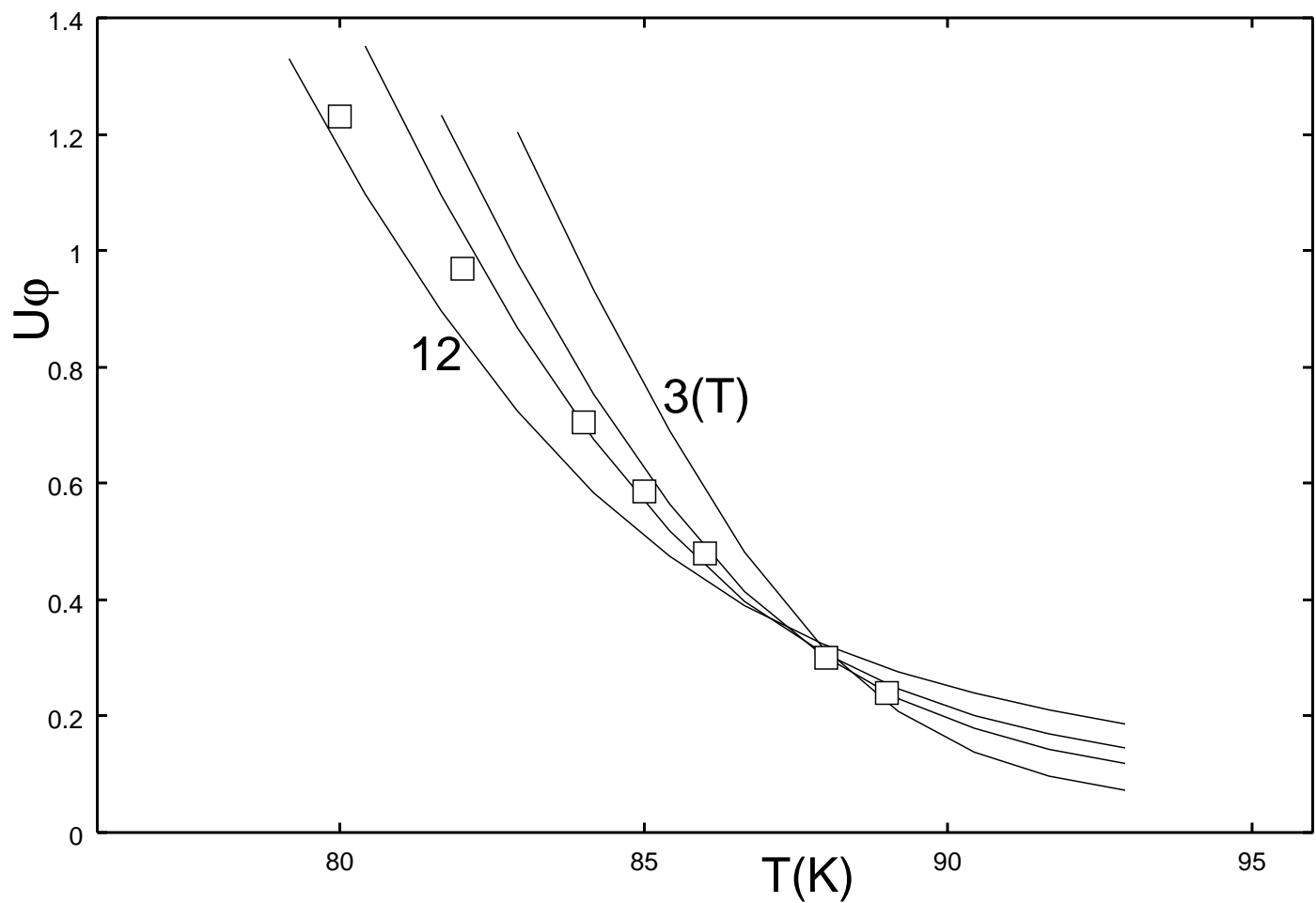


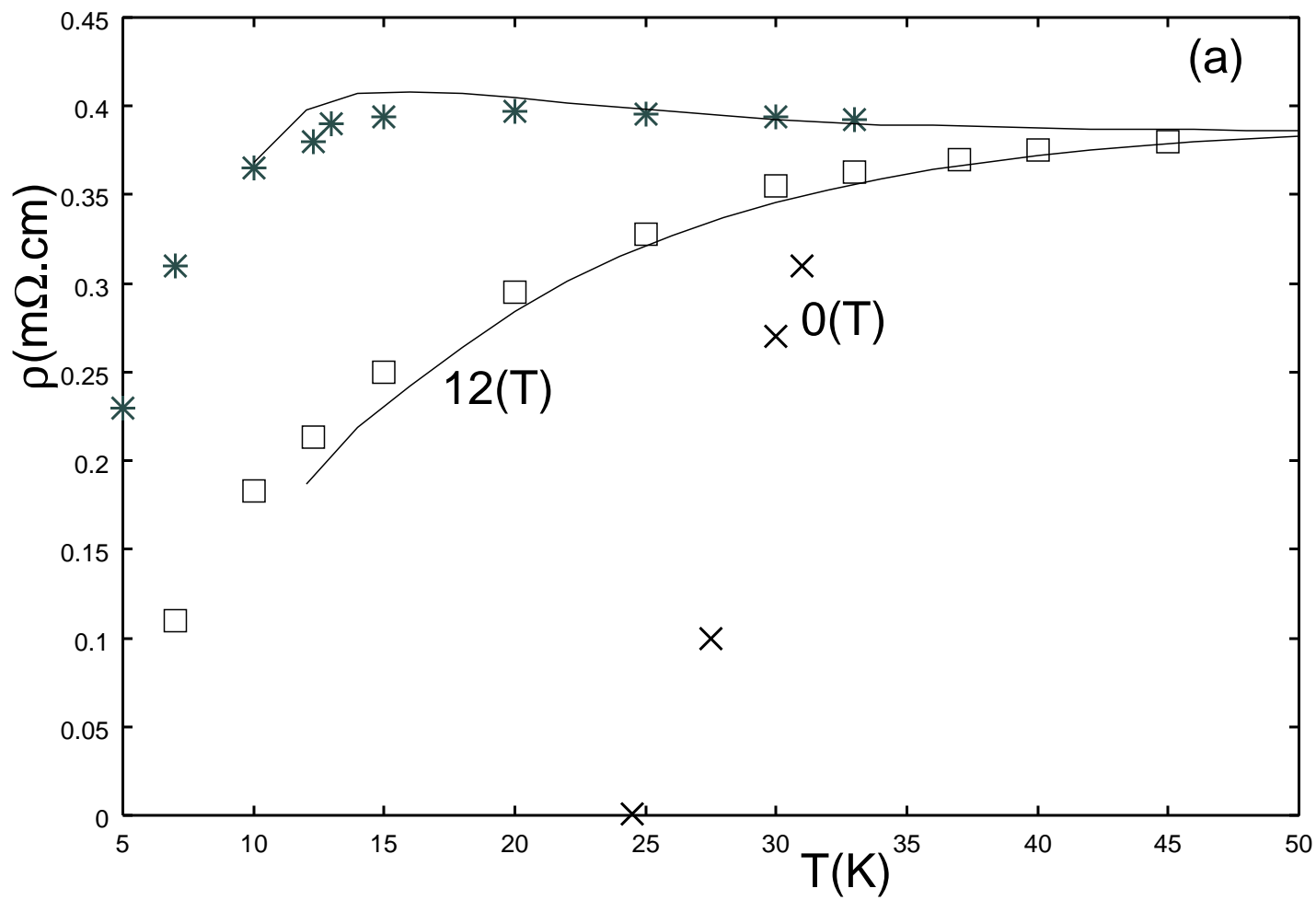
(d)

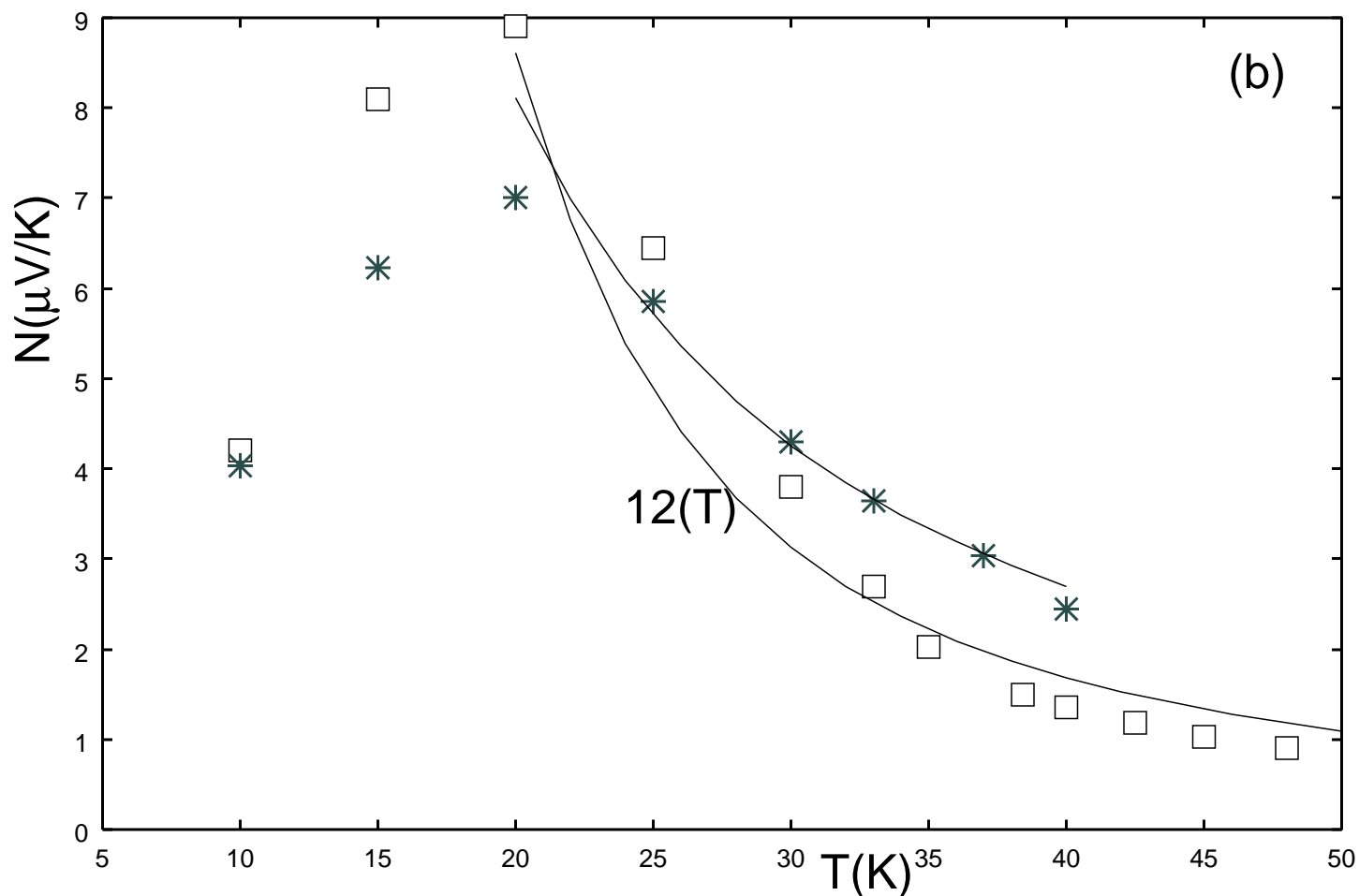


(e)

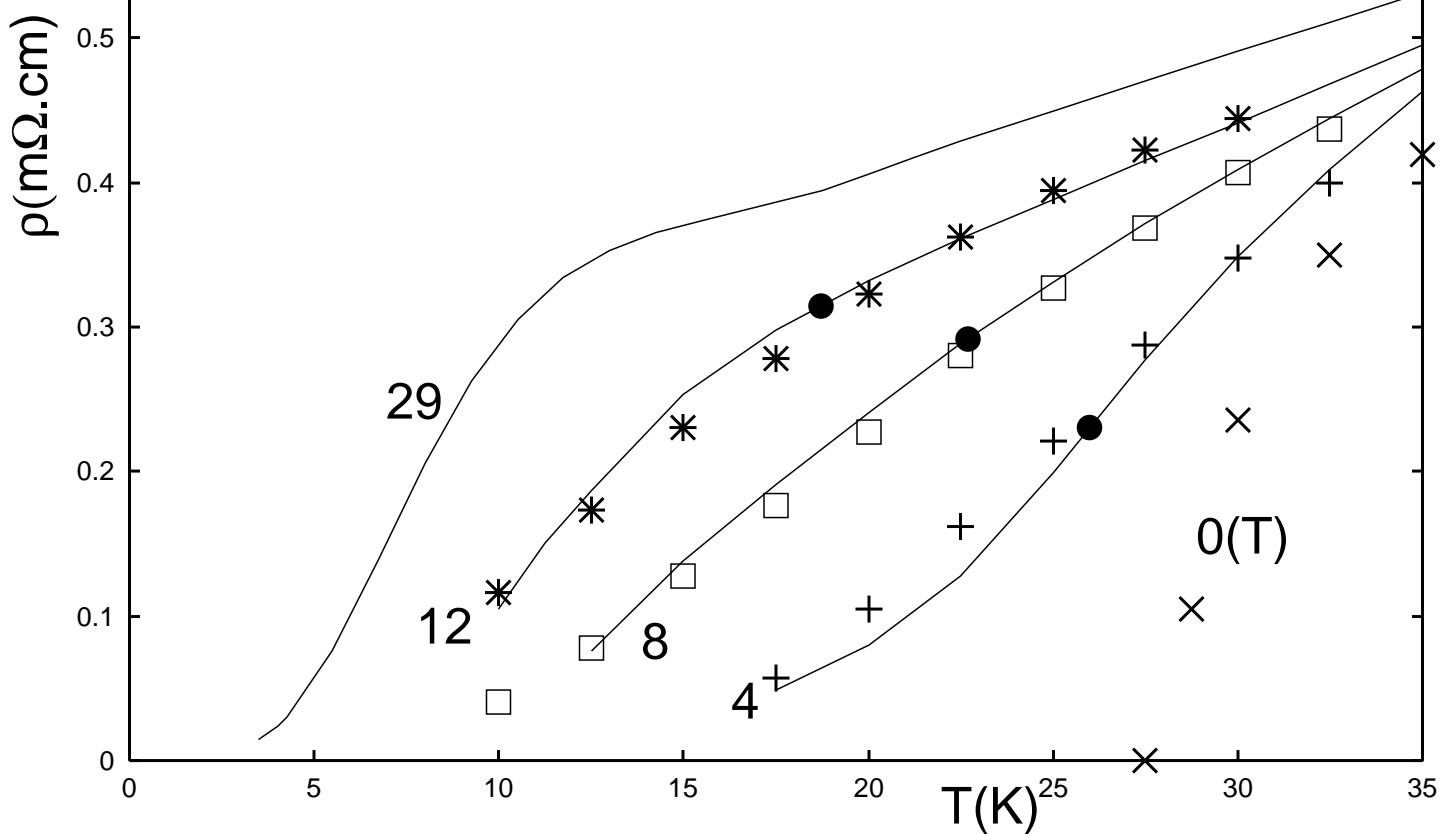
Rn/Rq	0.25	0.4	0.45	0.57	0.625	0.67
Bc*/Hc2	0.8	0.76	0.72	0.68	0.64	0.61
Rc/Rn	0.98	0.98	0.92	0.83	0.75	0.65



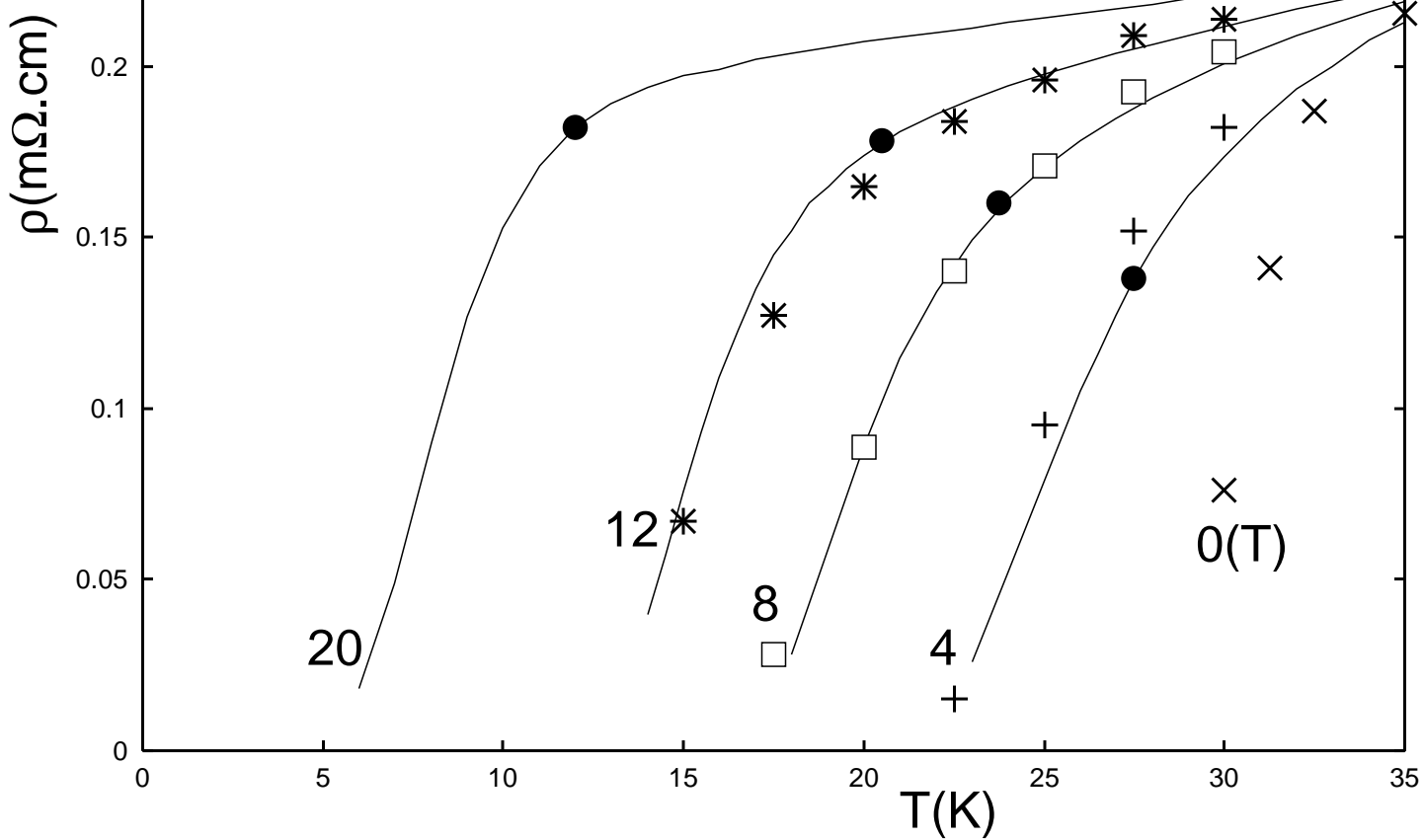


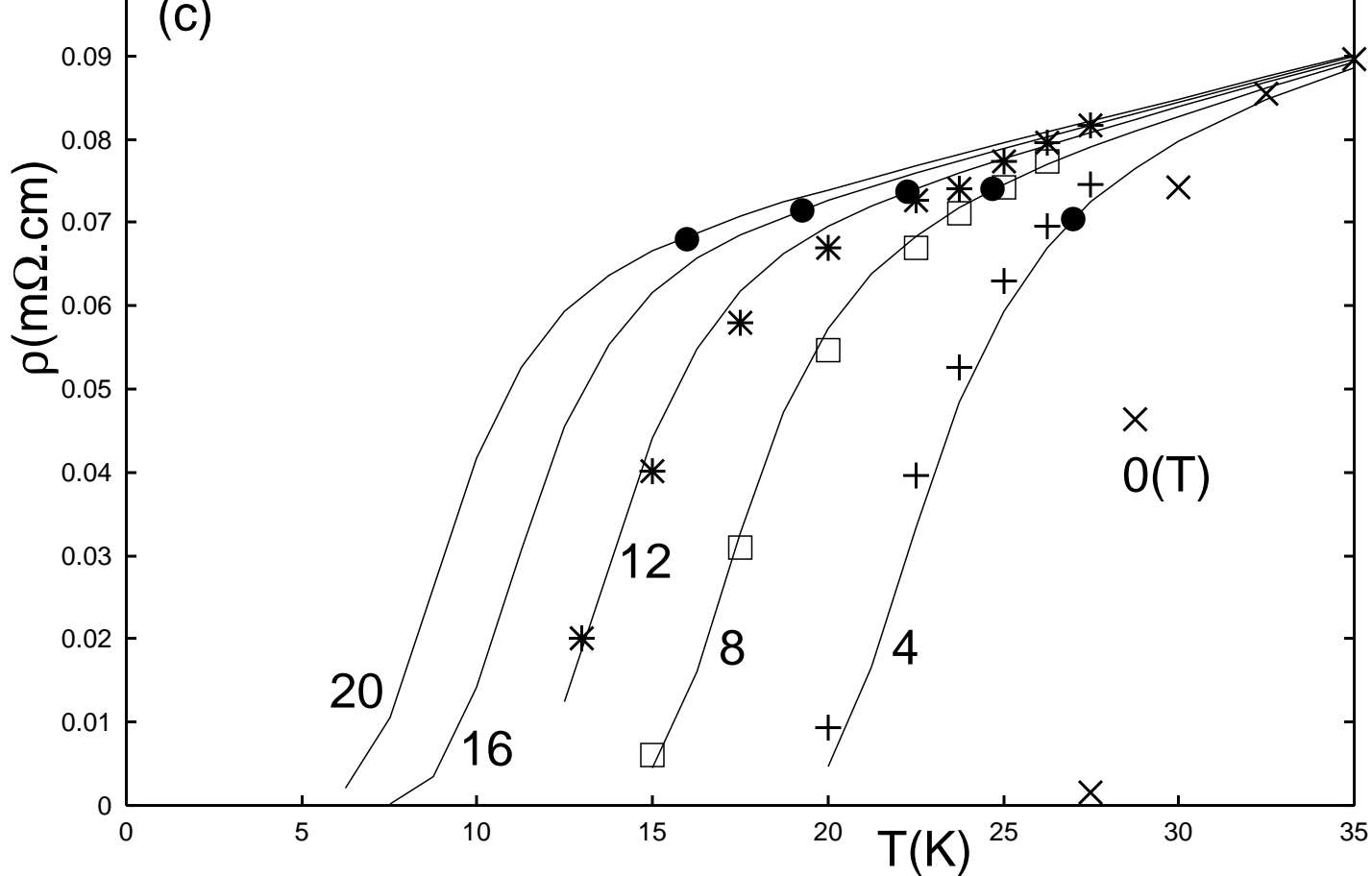


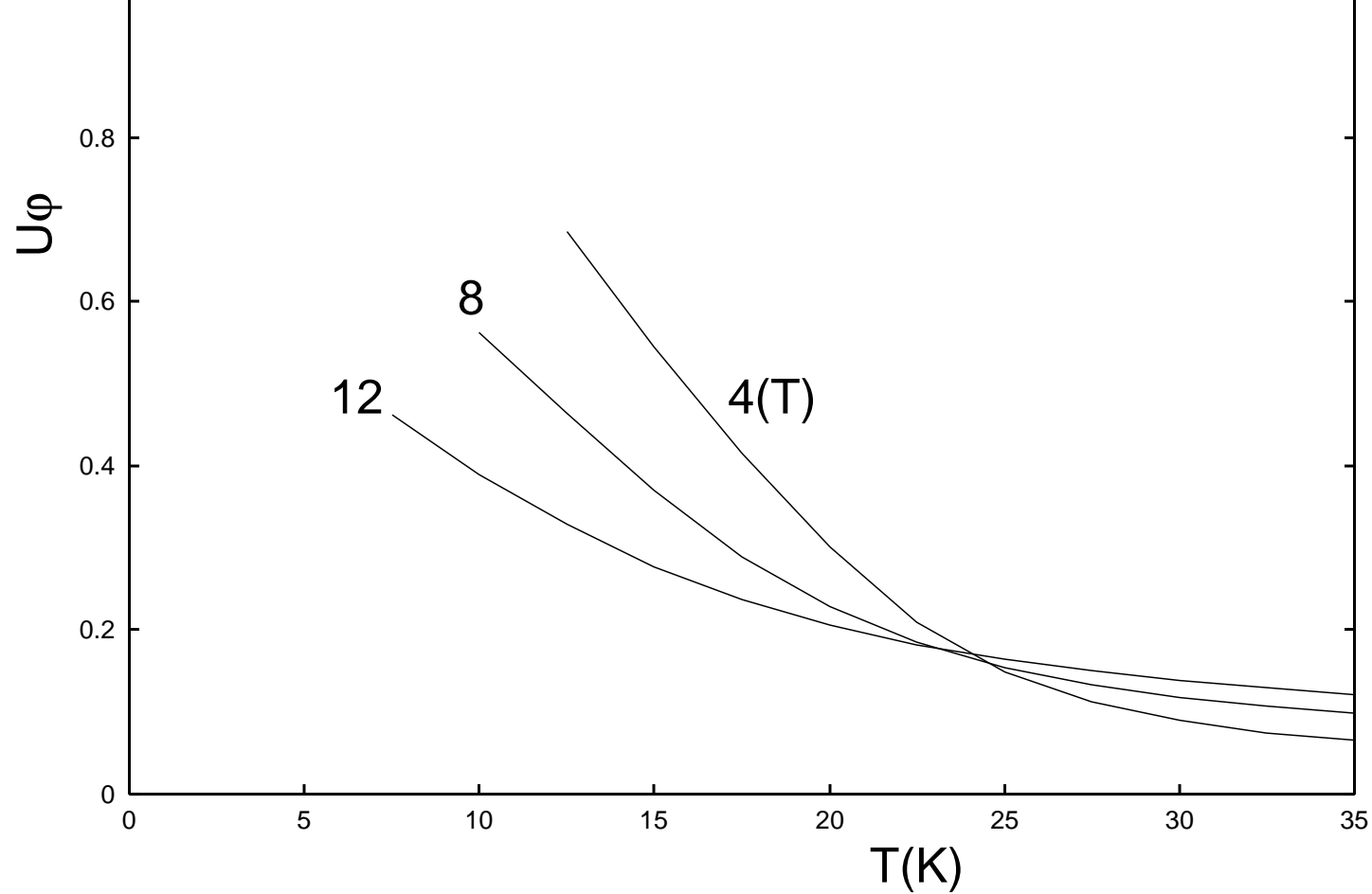
(a)



(b)







(a)

